Available online at www.sciencedirect.com
ScienceDirect

Comput. Methods Appl. Mech. Engrg. 370 (2020) 113264

Computer methods in applied mechanics and engineering

www.elsevier.com/locate/cma

Asymptotically compatible reproducing kernel collocation and meshfree integration for the peridynamic Navier equation

Yu Leng[a,*,1], Xiaochuan Tian[b,2], Nathaniel A. Trask[c,3], John T. Foster[a]

[a] Department of Petroleum and Geosystems Engineering, The University of Texas at Austin, Austin, TX 78712, United States
[b] Department of Mathematics, The University of Texas at Austin, Austin, TX 78712, United States
[c] Center for Computing Research, Sandia National Laboratories, Albuquerque, NM 87123, United States

Received 2 January 2020; received in revised form 29 June 2020; accepted 30 June 2020
Available online 18 July 2020

Abstract

In this work, we study reproducing kernel (RK) collocation method for peridynamic Navier equation. In the first part, we apply a linear RK approximation to both displacement and dilatation, and then back-substitute dilatation and solve the peridynamic Navier equation in a pure displacement form. The RK collocation scheme converges to the nonlocal limit for a fixed nonlocal interaction length and also to the local limit as nonlocal interactions vanish. The stability is shown by comparing the collocation scheme with the standard Galerkin scheme using Fourier analysis. In the second part, we apply the RK collocation to the quasi-discrete peridynamic Navier equation and show its convergence to the correct local limit when the ratio between the nonlocal length scale and the discretization parameter is fixed. The analysis is carried out on a special family of rectilinear Cartesian grids for the RK collocation method with a designated kernel with finite support. We assume the Lamé parameters satisfy $\lambda \geq \mu$ to avoid extra assumptions on the nonlocal kernel. Finally, numerical experiments are conducted to validate the theoretical results.

Keywords: Peridynamic Navier equation; Reproducing kernel collocation; Convergence analysis; Quasi-discrete nonlocal operator; Meshfree integration; Asymptotically compatible schemes

1. Introduction

Peridynamics is a nonlocal theory of continuum mechanics introduced by Silling in [1,2]. Peridynamic models avoid the use of spatial differentiation and they have attracted interest among researchers, especially for treating problems with fractures and material failure [3–5]. Mathematical analysis of the peridynamics models have been

* Corresponding author.
E-mail address: yu-leng@utexas.edu (Y. Leng).
[1] Current address: School of Mechanical Engineering, Purdue University, West Lafayette, IN 47906, United States.
[2] Current address: Department of Mathematics, University of California, San Diego, La Jolla, CA 92093, United States.
[3] Sandia National Laboratories is a multimission laboratory managed and operated by National Technology and Engineering Solutions of Sandia, LLC., a wholly owned subsidiary of Honeywell International, Inc., for the U.S. Department of Energy's National Nuclear Security Administration under contract DE-NA-0003525. This paper describes objective technical results and analysis. Any subjective views or opinions that might be expressed in the paper do not necessarily represent the views of the U.S. Department of Energy or the United States Government.

https://doi.org/10.1016/j.cma.2020.113264

carried out in [6–10] and it is well understood that the linear peridynamic Navier equation is well-posed. Many numerical methods have been developed to solve the peridynamic Naiver equation [11–19] and this is the main focus of our work. Other than [18] which is a variational method, the rest solve the nonlocal governing equation in the strong form without rigorous convergence analysis. To our knowledge, this is the first work that provides convergence analysis for non-variational numerical methods of the peridynamic Navier equation.

Nonlocal models introduce a length scale δ, called the *horizon* in peridynamics, which takes into account interactions over finite distances. As $\delta \to 0$, the nonlocal interactions vanish and the nonlocal model recovers its local limit, i.e., a partial differential equation. Numerical methods that preserve this limiting behavior in discrete form are called asymptotically compatible (AC) schemes [18,20–22]; many numerical methods for nonlocal models are not AC and may converge to the wrong local limit [21]. It is challenging to design AC schemes for nonlocal models. Another difficulty is the accurate evaluation of the nonlocal integral, which can be computationally prohibitive especially when the nonlocal kernels are singular, and it is often necessary to use a high-order Gaussian quadrature rule [14,23]. Many works have been done to address these two challenges [16,18,19,24–27].

Finite Element Method (FEM) [18] with linear basis functions is AC but the evaluation of the double integral [23,24,28] discourages the use of variational formulation for nonlocal models. Many mesh-free methods [16,17,26] for peridynamics, which use the volume of the particles as integration weights, are easy to implement but these methods do not converge to the correct local limit as the nonlocal length scale vanishes. A mesh-free integration scheme for the peridynamic Navier equation is introduced in [19], however, it lacks convergence analysis. The quadrature weights are calculated using the generalized moving least square technique and this mesh-free integration scheme converges to the correct local limit for nonlocal diffusion [29]. An important consequence of the mesh-free integration scheme is that it is straightforward to include "bond breaking" which provides a way to simulate fractures or material failure [19].

We have developed an AC RK collocation scheme for nonlocal diffusion models and introduced a quasi-discrete nonlocal diffusion operator using a mesh-free integration technique [29] to avoid using high-order Gauss quadrature rules and save the computational costs. RK collocation on this quasi-discrete nonlocal diffusion operator converges to the correct local limit. The purpose of this work is to extend the methodology to the peridynamic Navier equation.

First, we show RK collocation on the peridynamic Navier equation is AC. We use a similar strategy as in [29] to show the stability and consistency of the RK collocation method. The key idea for stability analysis is to compare the Fourier representation of the collocation scheme with the Galerkin scheme [29,30]. Similar ideas have been exploited in [31–34]. Since the Fourier symbol of the peridynamic Navier operator is a matrix instead of a scalar, the stability analysis is more involved for the peridynamic Navier equation than that of the nonlocal diffusion. Indeed, in order to simplify the discussion, we need to assume that the two Lamé parameters, λ and μ, satisfy the constraint $\lambda \geq \mu$. The uniform consistency of the numerical scheme, which is crucial to show that the scheme is AC, is established using the synchronized convergence property of the linear RK approximation with special RK support sizes [35–37]. Then, to obviate the need to use high-order Gauss quadrature rules and save computational costs, we introduce the quasi-discrete peridynamic Navier equation by carefully designing the integration weights. Convergence analysis of the RK collocation scheme on the quasi-discrete peridynamic Navier operator is presented when the ratio between horizon δ and the grid size $h_{\max}$ is fixed.

This paper is organized as follows. In Section 2, we introduce the peridynamic Navier equation with Dirichlet boundary conditions and also the quasi-discrete counterparts using finite summation of symmetric quadrature points in replacement of the integral. In Section 3, we present the RK collocation method with special choices of RK support size. Section 4 discusses the convergence analysis of the RK collocation method for the peridynamic Naiver equation and shows that this RK collocation scheme is AC. Then the convergence analysis of the collocation method on the quasi-discrete peridynamic Navier equation is presented in Section 5. Section 6 gives numerical examples to complement our theoretical analysis. Finally, we provide conclusions in Section 7.

2. Peridynamic Navier equation

In this section, we first introduce some notations that are used throughout the paper. The spatial dimension is denoted as d(d $=$ 2 or 3). An arbitrary point $\boldsymbol{x} \in \mathbb{R}^{\mathrm{d}}$ is expressed as $\boldsymbol{x} = (x_1, \ldots, x_{\mathrm{d}})$. A multi-index, $\boldsymbol{\alpha} = (\alpha_1, \ldots, \alpha_{\mathrm{d}})$, is a collection of d non-negative integers and its length is $|\boldsymbol{\alpha}| = \sum_{i=1}^{\mathrm{d}} \alpha_i$. As a consequence, we write $\boldsymbol{x}^{\boldsymbol{\alpha}} = x_1^{\alpha_1} \dots x_{\mathrm{d}}^{\alpha_{\mathrm{d}}}$ for a given $\boldsymbol{\alpha}$. We let $\Omega \subset \mathbb{R}^{\mathrm{d}}$ be an open bounded domain and then the corresponding interaction domain is defined as

$$\Omega_{\mathcal{I}_i} = \{\boldsymbol{x} \in \mathbb{R}^{\mathrm{d}} \backslash \Omega : \mathrm{dist}(\boldsymbol{x}, \Omega) \le i\delta\}, \quad i = 1 \text{ or } 2,$$

where δ is the nonlocal length scale and we denote $\Omega_{i\delta} = \Omega \cup \Omega_{\mathcal{I}_i}$, for $i = 1$ or 2. Ω is the domain of interest, and the nonlocal boundary condition is imposed on $\Omega_{\mathcal{I}_2}$ as a volumetric constraint [7].

Next, we present the state-based linearized peridynamic Navier equation introduced in [2,38], and then use the quasi-discrete nonlocal operators proposed in [29] to formulate the quasi-discrete counterparts. We differ in convention of notations from nonlocal vector calculus [12] which is more suited for variational formulations [7], but use instead notations for the bond-based peridynamics operator together with the nonlocal divergence and gradient operators as defined in [39–41]. These notations are more natural for the presentation of the collocation method that will be introduced in the next section.

2.1. Nonlocal operators

The linearized state-based peridynamic Navier operator consists of two parts; one is the bond-based peridynamic operator and the other is the composition of the nonlocal gradient and divergence operators. The bond-based peridynamic operator is defined, for a given vector-valued function $\boldsymbol{u}(\boldsymbol{x}) : \mathbb{R}^{\mathrm{d}} \to \mathbb{R}^{\mathrm{d}}$, as

$$\mathcal{L}_\delta^B \boldsymbol{u}(\boldsymbol{x}) = \int_{\mathbb{R}^{\mathrm{d}}} \rho_\delta(|\boldsymbol{y}-\boldsymbol{x}|) \frac{\boldsymbol{y}-\boldsymbol{x}}{|\boldsymbol{y}-\boldsymbol{x}|} \otimes \frac{\boldsymbol{y}-\boldsymbol{x}}{|\boldsymbol{y}-\boldsymbol{x}|} (\boldsymbol{u}(\boldsymbol{y}) - \boldsymbol{u}(\boldsymbol{x})) d\boldsymbol{y}, \tag{1}$$

where $\rho_\delta(|\boldsymbol{y}-\boldsymbol{x}|)$ is the nonlocal kernel. We assume the nonlocal kernel is non-negative and symmetric, and has the following scaling,

$$\rho_\delta(|\boldsymbol{s}|) = \frac{1}{\delta^{\mathrm{d}+2}} \rho\left(\frac{|\boldsymbol{s}|}{\delta}\right), \tag{2}$$

where $\rho(|\boldsymbol{s}|)$ is a non-negative and non-increasing function with compact support in B_1 (for the rest of the paper, we denote B_δ as $B_\delta(\boldsymbol{0})$, a ball of radius δ about $\boldsymbol{0}$), and it has a bounded second order moment, i.e.,

$$\int_{B_1} \rho(|\boldsymbol{s}|)|\boldsymbol{s}|^2 d\boldsymbol{s} = \mathrm{d}. \tag{3}$$

Notice that since ρ_δ is supported on B_δ, the integration in Eq. (1) is in fact over the ball, $B_\delta(\boldsymbol{x})$, for any $\boldsymbol{x} \in \mathbb{R}^{\mathrm{d}}$. The weighted volume $m(\boldsymbol{x})$ is defined as

$$m(\boldsymbol{x}) = \int_{\mathbb{R}^{\mathrm{d}}} \rho_\delta(|\boldsymbol{y}-\boldsymbol{x}|)|\boldsymbol{y}-\boldsymbol{x}|^2 d\boldsymbol{y}. \tag{4}$$

From Eqs. (2)–(4), it is easy to see that $m(\boldsymbol{x}) = \mathrm{d}$ for all $\boldsymbol{x}$. We remark that the weighted volume defined here as Eq. (4) is a scaled form of the definition in [1,2,42]. Next, the nonlocal divergence operator $\mathcal{D}_\delta$ is defined as [39,40],

$$\mathcal{D}_\delta \boldsymbol{u}(\boldsymbol{x}) = \int_{\mathbb{R}^{\mathrm{d}}} \rho_\delta(|\boldsymbol{y}-\boldsymbol{x}|)(\boldsymbol{y}-\boldsymbol{x}) \cdot (\boldsymbol{u}(\boldsymbol{y}) + \boldsymbol{u}(\boldsymbol{x})) d\boldsymbol{y},$$

and in the sense of principle value, $\mathcal{D}_\delta$ can also be written as

$$\mathcal{D}_\delta \boldsymbol{u}(\boldsymbol{x}) = \int_{\mathbb{R}^{\mathrm{d}}} \rho_\delta(|\boldsymbol{y}-\boldsymbol{x}|)(\boldsymbol{y}-\boldsymbol{x}) \cdot (\boldsymbol{u}(\boldsymbol{y}) - \boldsymbol{u}(\boldsymbol{x})) d\boldsymbol{y}. \tag{5}$$

As a consequence of the nonlocal divergence operator, nonlocal dilatation $\theta(\boldsymbol{x})$ is given as,

$$\theta(\boldsymbol{x}) = \frac{\mathrm{d}}{m(\boldsymbol{x})} \mathcal{D}_\delta \boldsymbol{u}(\boldsymbol{x}). \tag{6}$$

For a scalar-valued function $\theta(\boldsymbol{x}) : \mathbb{R}^{\mathrm{d}} \to \mathbb{R}$, the nonlocal gradient operator $\mathcal{G}_\delta$ is defined by

$$\mathcal{G}_\delta \theta(\boldsymbol{x}) = \int_{\mathbb{R}^{\mathrm{d}}} \rho_\delta(|\boldsymbol{y}-\boldsymbol{x}|)(\boldsymbol{y}-\boldsymbol{x})(\theta(\boldsymbol{y}) - \theta(\boldsymbol{x})) d\boldsymbol{y}. \tag{7}$$

Finally, we have the linearized state-based peridynamic Navier operator,

$$\mathcal{L}_\delta^S \boldsymbol{u}(\boldsymbol{x}) = \frac{C_\alpha \mu}{m(\boldsymbol{x})} \mathcal{L}_\delta^B \boldsymbol{u}(\boldsymbol{x}) + \frac{C_\beta \mathrm{d}(\lambda - \mu)}{(m(\boldsymbol{x}))^2} \mathcal{G}_\delta \mathcal{D}_\delta \boldsymbol{u}(\boldsymbol{x}), \tag{8}$$

where C_α and C_β are scaling parameters which will be given shortly, and λ and μ are Lamé parameters which are assumed to be constant in this work. The static peridynamic Navier equation with homogeneous Dirichlet boundary condition can be formulated as

$$\begin{cases} -\mathcal{L}_\delta^S \boldsymbol{u}(\boldsymbol{x}) = \boldsymbol{f}(\boldsymbol{x}), & \boldsymbol{x} \in \Omega, \\ \quad \boldsymbol{u}(\boldsymbol{x}) = \boldsymbol{0}, & \boldsymbol{x} \in \Omega_{\mathcal{I}_2}. \end{cases} \tag{9}$$

We remark that because the kernel $\rho_\delta(|\boldsymbol{s}|)$ is compactly supported in a ball of radius δ, it is only necessary to impose volumetric constraint on $\Omega_{\mathcal{I}_2}$. Even though we have defined $\boldsymbol{u}(\boldsymbol{x})$ on $\mathbb{R}^{\mathrm{d}}$, we do not need the values of $\boldsymbol{u}$ on $\mathbb{R}^{\mathrm{d}} \backslash \Omega_{2\delta}$ to define Eq. (9). By introducing $p = (\lambda - \mu)\theta$, we can rewrite Eq. (9) in a mixed form, as follows,

$$\begin{cases} -\dfrac{C_\alpha \mu}{m(\boldsymbol{x})} \mathcal{L}_\delta^B \boldsymbol{u}(\boldsymbol{x}) - \dfrac{C_\beta}{m(\boldsymbol{x})} \mathcal{G}_\delta p(\boldsymbol{x}) = \boldsymbol{f}(\boldsymbol{x}), & \boldsymbol{x} \in \Omega, \\ \dfrac{\mathrm{d}\,(\lambda - \mu)}{m(\boldsymbol{x})} \mathcal{D}_\delta \boldsymbol{u}(\boldsymbol{x}) - p(\boldsymbol{x}) = 0, & \boldsymbol{x} \in \Omega_\delta, \\ \boldsymbol{u}(\boldsymbol{x}) = \boldsymbol{0}, & \boldsymbol{x} \in \Omega_{\mathcal{I}_2}. \end{cases} \tag{10}$$

The local limit of $\mathcal{L}_\delta^S$ is denoted as $\mathcal{L}_0^S$ when $\delta \to 0$ [9]. We select $C_\alpha = 30, C_\beta = 3$ for three-dimensional linear elasticity and $C_\alpha = 16, C_\beta = 2$ for two-dimensional plane strain, then

$$\mathcal{L}_0^S \boldsymbol{u}(\boldsymbol{x}) = \mu \mathrm{div}(\nabla \boldsymbol{u}(\boldsymbol{x})) + (\mu + \lambda) \nabla \mathrm{div} \boldsymbol{u}(\boldsymbol{x}), \quad \forall \boldsymbol{x} \in \Omega,$$

and the $\delta \to 0$ limit of Eq. (9) becomes

$$\begin{cases} -\mathcal{L}_0^S \boldsymbol{u} = \boldsymbol{f}, & \text{in } \Omega, \\ \quad \boldsymbol{u} = \boldsymbol{0}, & \text{on } \partial\Omega. \end{cases} \tag{11}$$

Define the "energy space" $\mathcal{S}_\delta$ as

$$\mathcal{S}_\delta := \left\{ \boldsymbol{u} \in L^2(\mathbb{R}^{\mathrm{d}}; \mathbb{R}^{\mathrm{d}}) : \int_{\mathbb{R}^{\mathrm{d}}} \int_{\mathbb{R}^{\mathrm{d}}} \rho_\delta(|\boldsymbol{y} - \boldsymbol{x}|) (\mathrm{Tr}(\mathcal{D}^* \boldsymbol{u})(\boldsymbol{y}, \boldsymbol{x}))^2 d\boldsymbol{y} d\boldsymbol{x} < \infty \right\},$$

where $\mathrm{Tr}(\mathcal{D}^* \boldsymbol{u})$ is the trace of the operator $\mathcal{D}^*$ defined in [8,10] as

$$\mathcal{D}^* \boldsymbol{u}(\boldsymbol{y}, \boldsymbol{x}) := (\boldsymbol{u}(\boldsymbol{y}) - \boldsymbol{u}(\boldsymbol{x})) \otimes \frac{\boldsymbol{y} - \boldsymbol{x}}{|\boldsymbol{y} - \boldsymbol{x}|}.$$

Then the weak formulation of Eq. (9) can be formed with solutions in the constrained energy space

$$\mathcal{S}_{c,\delta}(\Omega) := \{ \boldsymbol{u} \in \mathcal{S}_\delta : \boldsymbol{u}(\boldsymbol{x}) = \boldsymbol{0}, \forall \boldsymbol{x} \in \mathbb{R}^{\mathrm{d}} \backslash \Omega \}.$$

It is shown in [10] that the static peridynamic Navier equation (Eq. (9)) is well-posed as a result of the Lax–Milgram theorem and nonlocal Poincaré inequality. In fact, the nonlocal Poincaré inequality in [9,10] gives the following uniform stability result.

Theorem 2.1. *Assume that $\widetilde{\Omega} \subset \mathbb{R}^{\mathrm{d}}$ is an open bounded connected domain and $\delta \in (0, \delta_0]$ for some $\delta_0 > 0$. Let $\boldsymbol{u} \in \mathcal{S}_\delta$ and $\boldsymbol{u}|_{\mathbb{R}^{\mathrm{d}} \backslash \widetilde{\Omega}} = \boldsymbol{0}$. Then the bilinear form $(-\mathcal{L}_\delta^S \boldsymbol{u}, \boldsymbol{u})$ is an inner product and there exists a constant $C > 0$ which depends on δ_0 and $\widetilde{\Omega}$, such that for all $\boldsymbol{u} \in \mathcal{S}_\delta$ with $\boldsymbol{u}|_{\mathbb{R}^{\mathrm{d}} \backslash \widetilde{\Omega}} = \boldsymbol{0}$, we have*

$$|(-\mathcal{L}_\delta^S \boldsymbol{u}, \boldsymbol{u})| \geq C \|\boldsymbol{u}\|^2_{L^2(\mathbb{R}^{\mathrm{d}}; \mathbb{R}^{\mathrm{d}})}.$$

2.2. Quasi-discrete nonlocal operators

As introduced in [29], we use a finite number of symmetric quadrature points $\boldsymbol{s}$ in the horizon to evaluate the integral such that the weighted volume defined in Eq. (4) is exact,

$$m(\boldsymbol{x}) = \sum_{\boldsymbol{s} \in B_\delta^\epsilon(\boldsymbol{0})} \omega_\delta(\boldsymbol{s}) \rho_\delta(|\boldsymbol{s}|) |\boldsymbol{s}|^2 = \mathrm{d}, \tag{12}$$

where $\omega_\delta(\boldsymbol{s})$ is the quadrature weight at quadrature point $\boldsymbol{s}$ and satisfies the following assumptions

$$\omega_\delta(\boldsymbol{s}) \geq 0 \text{ and } \omega_\delta(\boldsymbol{s}) = \omega_\delta(|\boldsymbol{s}|), \tag{13}$$

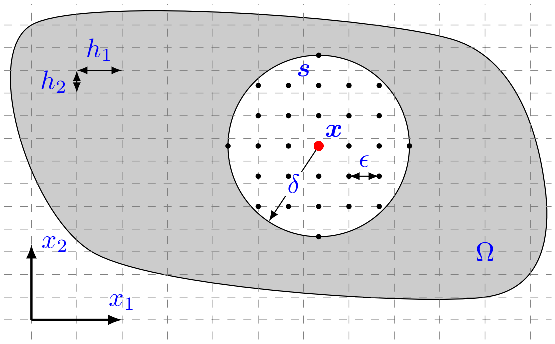

Fig. 1. Quadrature points (black dots) are shown in the horizon of an arbitrary point $\boldsymbol{x} \in \Omega$. The dashed lines form the RK collocation grid which will be introduced in Section 3. (For interpretation of the references to color in this figure legend, the reader is referred to the web version of this article.)

and $B_\delta^\epsilon(\mathbf{0})$ is a finite collection of symmetric quadrature points $\boldsymbol{s}$ in the ball of radius δ about $\mathbf{0}$. The notation ϵ can be seen as the discretization parameter of the ball B_δ and we assume $\epsilon_1 := \epsilon/\delta$ is a fixed number. We use B_δ^ϵ to denote $B_\delta^\epsilon(\mathbf{0})$ for the rest of the paper. An example of quadrature points in the horizon of an arbitrary point $\boldsymbol{x} \in \Omega$ is shown in Fig. 1.

Due to the scaling of the nonlocal kernel $\rho_\delta(|\boldsymbol{s}|)$, see Eq. (2), we also have the scaling of the quadrature weights $\omega_\delta(\boldsymbol{s})$ as

$$\omega_\delta(\boldsymbol{s}) = \delta^{\mathrm{d}} \omega\left(\frac{\boldsymbol{s}}{\delta}\right),$$

where $\omega(\boldsymbol{s})$ is the quadrature weight at $\boldsymbol{s} \in B_1^{\epsilon_1}$ and $\epsilon_1 = \epsilon/\delta$ can be seen as the discretization parameter of the unit ball. As a consequence, we have a discrete version of Eq. (3) as,

$$\sum_{\boldsymbol{s} \in B_1^{\epsilon_1}} \omega(\boldsymbol{s})\rho(|\boldsymbol{s}|)|\boldsymbol{s}|^2 = \mathrm{d}. \tag{14}$$

However, unlike the nonlocal diffusion in [29], Eq. (14) alone is not sufficient for the construction of a consistent quasi-discrete peridynamic Navier operator and additional constraints are necessary. We will now define the quasi-discrete peridynamic Navier operator and complete the constraints on quadrature weights afterwards.

We now formulate the quasi-discrete counterparts of the nonlocal operators defined in the previous subsection. The quasi-discrete bond-based peridynamic operator $\mathcal{L}_{\delta,\epsilon}^B$ acting on $\boldsymbol{u}(\boldsymbol{x}) : \mathbb{R}^{\mathrm{d}} \to \mathbb{R}^{\mathrm{d}}$ is defined as

$$\mathcal{L}_{\delta,\epsilon}^B \boldsymbol{u}(\boldsymbol{x}) = \sum_{\boldsymbol{s} \in B_\delta^\epsilon} \omega_\delta(\boldsymbol{s})\rho_\delta(|\boldsymbol{s}|)\frac{\boldsymbol{s}}{|\boldsymbol{s}|} \otimes \frac{\boldsymbol{s}}{|\boldsymbol{s}|}(\boldsymbol{u}(\boldsymbol{x}+\boldsymbol{s}) - \boldsymbol{u}(\boldsymbol{x})). \tag{15}$$

Similarly, the quasi-discrete nonlocal divergence operator $\mathcal{D}_\delta^\epsilon$ is formulated as,

$$\mathcal{D}_\delta^\epsilon \boldsymbol{u}(\boldsymbol{x}) = \sum_{\boldsymbol{s} \in B_\delta^\epsilon} \omega_\delta(\boldsymbol{s})\rho_\delta(|\boldsymbol{s}|)\, \boldsymbol{s} \cdot (\boldsymbol{u}(\boldsymbol{x}+\boldsymbol{s}) - \boldsymbol{u}(\boldsymbol{x})), \tag{16}$$

A direct consequence of the quasi-discrete nonlocal divergence operator is the nonlocal dilatation,

$$\theta^\epsilon(\boldsymbol{x}) = \frac{\mathrm{d}}{m(\boldsymbol{x})}\mathcal{D}_\delta^\epsilon \boldsymbol{u}(\boldsymbol{x}), \tag{17}$$

where we have abused the definition of nonlocal dilatation. We remark that θ^ϵ is a continuous function with respect to $\boldsymbol{x}$ and its definition differs from Eq. (6). We also have the quasi-discrete nonlocal gradient operator,

$$\mathcal{G}_\delta^\epsilon \theta^\epsilon(\boldsymbol{x}) = \sum_{\boldsymbol{s} \in B_\delta^\epsilon} \omega_\delta(\boldsymbol{s})\rho_\delta(|\boldsymbol{s}|)\, \boldsymbol{s}\, (\theta^\epsilon(\boldsymbol{x}+\boldsymbol{s}) - \theta^\epsilon(\boldsymbol{x})), \tag{18}$$

Finally, we arrive at the linearized state-based quasi-discrete peridynamic Navier operator,

$$\mathcal{L}_{\delta,\epsilon}^S \boldsymbol{u}(\boldsymbol{x}) = \frac{C_\alpha \mu}{m(\boldsymbol{x})}\mathcal{L}_{\delta,\epsilon}^B \boldsymbol{u}(\boldsymbol{x}) + \frac{C_\beta \mathrm{d}(\lambda - \mu)}{(m(\boldsymbol{x}))^2}\mathcal{G}_\delta^\epsilon \mathcal{D}_\delta^\epsilon \boldsymbol{u}(\boldsymbol{x}), \tag{19}$$

and the static peridynamic Navier equation can be reformulated as

$$\begin{cases} -\mathcal{L}^{S}_{\delta,\epsilon}\boldsymbol{u}(\boldsymbol{x}) = \boldsymbol{f}(\boldsymbol{x}), & \boldsymbol{x} \in \Omega, \\ \quad\quad \boldsymbol{u}(\boldsymbol{x}) = \boldsymbol{0}, & \boldsymbol{x} \in \Omega_{\mathcal{I}_2}. \end{cases} \tag{20}$$

Similar to Eq. (10), if we let $p = (\lambda - \mu)\theta^{\epsilon}$, we can rewrite Eq. (20) as

$$\begin{cases} -\dfrac{C_\alpha\,\mu}{m(\boldsymbol{x})}\mathcal{L}^{B}_{\delta,\epsilon}\boldsymbol{u}(\boldsymbol{x}) - \dfrac{C_\beta}{m(\boldsymbol{x})}\mathcal{G}^{\epsilon}_{\delta}\, p(\boldsymbol{x}) = \boldsymbol{f}(\boldsymbol{x}), & \boldsymbol{x} \in \Omega, \\ \dfrac{\mathrm{d}\,(\lambda-\mu)}{m(\boldsymbol{x})}\mathcal{D}^{\epsilon}_{\delta}\boldsymbol{u}(\boldsymbol{x}) - p(\boldsymbol{x}) = 0, & \boldsymbol{x} \in \Omega_{\delta}, \\ \boldsymbol{u}(\boldsymbol{x}) = \boldsymbol{0}, & \boldsymbol{x} \in \Omega_{\mathcal{I}_2}. \end{cases} \tag{21}$$

To guarantee consistency, we require the quasi-discrete peridynamic Navier operator to possess the *quadratic exactness* property, i.e., for $\boldsymbol{u}$ being any quadratic polynomials,

$$\mathcal{L}^{S}_{\delta,\epsilon}\boldsymbol{u} = \mathcal{L}^{S}_{\delta}\boldsymbol{u}\,. \tag{22}$$

This condition also ensures that the quasi-discrete peridynamic Navier operator $\mathcal{L}^{S}_{\delta,\epsilon}$ converges to $\mathcal{L}^{S}_{0}$ as δ goes to 0. Eq. (22) is fulfilled if and only if

$$\sum_{\boldsymbol{s}\in B_1^{\epsilon_1}} \omega(\boldsymbol{s})\rho(|\boldsymbol{s}|)\frac{s_i^2 s_j^2}{|\boldsymbol{s}|^2} = \int_{\boldsymbol{s}\in B_1} \rho(|\boldsymbol{s}|)\frac{s_i^2 s_j^2}{|\boldsymbol{s}|^2}d\boldsymbol{s}, \tag{23}$$

for all $i, j = 1, \ldots, \mathrm{d}$. It is easy to see that the quantities in Eq. (23) are bounded because of Eq. (3) and the constraint given by Eq. (14) is only a subset of the constraints presented by Eq. (23).

3. RK collocation method

In this section, we discuss the RK collocation method and formulate the collocation scheme for the peridynamic Navier equation (9) and its quasi-discrete counterpart Eq. (20). First, we introduce the collocation grid. Let $\square$ be a rectilinear Cartesian grid on $\mathbb{R}^{\mathrm{d}}$,

$$\square := \{\boldsymbol{x}_{\boldsymbol{k}} := \boldsymbol{k} \odot \boldsymbol{h} \mid \boldsymbol{k} \in \mathbb{Z}^{\mathrm{d}}\},$$

where $\odot$ denotes component-wise multiplication, i.e.,

$$\boldsymbol{k} \odot \boldsymbol{h} = (k_1 h_1, \ldots, k_{\mathrm{d}} h_{\mathrm{d}}),$$

for $\boldsymbol{k} = (k_1, \ldots, k_{\mathrm{d}})$, and $\boldsymbol{h} = (h_1, \ldots, h_{\mathrm{d}})$ where h_j is the discretization parameter in the jth dimension. Similarly, component-wise division is denoted as $\oslash$:

$$\boldsymbol{k} \oslash \boldsymbol{h} = \left(\frac{k_1}{h_1}, \ldots, \frac{k_{\mathrm{d}}}{h_{\mathrm{d}}}\right).$$

We remark that the grid size h_j can vary for different j and we let $h_{\max} = \max_{j=1}^{\mathrm{d}} h_j$ and $h_{\min} = \min_{j=1}^{\mathrm{d}} h_j$. For instance, in two dimension, rectangular grids are allowed. In addition, we assume that the grid $\square$ is quasi-uniform such that $\boldsymbol{h}$ can be rewritten as

$$\boldsymbol{h} = h_{\max}\hat{\boldsymbol{h}}\,, \tag{24}$$

where $\hat{\boldsymbol{h}}$ is a fixed vector with its maximum component being 1 and the minimum component being bounded below.

Next, we let $S(\square)$ be the trial space equipped with RK basis on $\square$, i.e., $S(\square) = \mathrm{span}\{\Psi_{\boldsymbol{k}}(\boldsymbol{x}) \mid \boldsymbol{k} \in \mathbb{Z}^{\mathrm{d}}\}$. The RK basis function $\Psi_{\boldsymbol{k}}(\boldsymbol{x})$ is given as

$$\Psi_{\boldsymbol{k}}(\boldsymbol{x}) = \prod_{j=1}^{\mathrm{d}} \phi\left(\frac{|x_j - x_{k_j}|}{2h_j}\right), \tag{25}$$

where $x_{k_j} = k_j h_j$ is the jth component of $\boldsymbol{x_k}$, $2h_j$ is the RK support in the jth dimension, and $\phi(x)$ is the cubic B-spline function

$$\phi(x) = \begin{cases} \frac{2}{3} - 4x^2 + 4x^3, & 0 \le x \le \frac{1}{2}, \\ \frac{4}{3}(1-x)^3, & \frac{1}{2} \le x \le 1, \\ 0, & \text{otherwise.} \end{cases} \tag{26}$$

Remark 3.1. For the simplicity of presentation, we choose the RK support size $\boldsymbol{a} = a_0 \boldsymbol{h}$ where $a_0 = 2$ in this work but the analysis works for a general even number a_0 [29,43].

Thus, the RK basis function can reproduce linear polynomials [36,43,44], i.e.,

$$\sum_{\boldsymbol{k} \in \mathbb{Z}^{\mathrm{d}}} \Psi_{\boldsymbol{k}}(\boldsymbol{x}) \boldsymbol{x}_{\boldsymbol{k}}^{\boldsymbol{\alpha}} = \boldsymbol{x}^{\boldsymbol{\alpha}}, \text{ for } |\boldsymbol{\alpha}| = 1. \tag{27}$$

For $u \in C^0(\mathbb{R}^{\mathrm{d}}; \mathbb{R})$, we define the restriction to $\square$ by

$$r^h u := (u(\boldsymbol{x_k}))_{\boldsymbol{k} \in \mathbb{Z}^{\mathrm{d}}},$$

and the restriction to $(\square \cap \Omega)$ as

$$r_\Omega^h u := (u(\boldsymbol{x_k})), \quad \boldsymbol{x_k} \in (\square \cap \Omega),$$

where $\square \cap \Omega$ is the collection of grid points that only reside in Ω. For a sequence $(u_{\boldsymbol{k}})_{\boldsymbol{k} \in \mathbb{Z}^{\mathrm{d}}}$ on $\mathbb{R}$, the RK interpolation operator is defined by

$$i^h(u_{\boldsymbol{k}}) := \sum_{\boldsymbol{k} \in \mathbb{Z}^{\mathrm{d}}} \Psi_{\boldsymbol{k}}(\boldsymbol{x}) u_{\boldsymbol{k}}.$$

For $j = 1, \ldots, \mathrm{d}$, we denote $u_j(\boldsymbol{x}) : \mathbb{R}^{\mathrm{d}} \to \mathbb{R}$ the jth component of a vector field $\boldsymbol{u}(\boldsymbol{x}) = [u_1(\boldsymbol{x}), \ldots, u_{\mathrm{d}}(\boldsymbol{x})]^T$ and denote $(u_{j,\boldsymbol{k}})_{\boldsymbol{k} \in \mathbb{Z}^{\mathrm{d}}}$ the jth component of the vector sequence

$$(\boldsymbol{u_k})_{\boldsymbol{k} \in \mathbb{Z}^{\mathrm{d}}} = [(u_{1,\boldsymbol{k}})_{\boldsymbol{k} \in \mathbb{Z}^{\mathrm{d}}}, \ldots, (u_{\mathrm{d},\boldsymbol{k}})_{\boldsymbol{k} \in \mathbb{Z}^{\mathrm{d}}}]^T.$$

Then the RK interpolation operator i^h acting on $(\boldsymbol{u_k})_{\boldsymbol{k} \in \mathbb{Z}^{\mathrm{d}}}$ is naturally understood as $i^h(\boldsymbol{u_k}) := [i^h(u_{1,\boldsymbol{k}}), \ldots, i^h(u_{\mathrm{d},\boldsymbol{k}})]^T$. Now we let

$$\Pi^h := i^h r^h$$

be the interpolation projector mapping from $C^0(\mathbb{R}^{\mathrm{d}})$ to $S(\square)$. Therefore, we can write

$$\Pi^h \boldsymbol{u} := [\Pi^h u_1, \ldots, \Pi^h u_{\mathrm{d}}]^T,$$

where $\Pi^h u_j(\boldsymbol{x})$ is the RK approximation of $u_j(\boldsymbol{x})$,

$$\Pi^h u_j(\boldsymbol{x}) = \sum_{\boldsymbol{k} \in \mathbb{Z}^{\mathrm{d}}} \Psi_{\boldsymbol{k}}(\boldsymbol{x}) u_j(\boldsymbol{x_k}).$$

Finally, we apply RK approximation on both $\boldsymbol{u}$ and θ, back-substitute θ into the first equation of Eq. (10) and obtain

$$\mathcal{L}_\delta^S \Pi^h \boldsymbol{u} = \frac{C_\alpha \mu}{m(\boldsymbol{x})} \mathcal{L}_\delta^B \Pi^h \boldsymbol{u} + \frac{C_\beta \mathrm{d}(\lambda - \mu)}{(m(\boldsymbol{x}))^2} \mathcal{G}_\delta \Pi^h (\mathcal{D}_\delta \Pi^h \boldsymbol{u}).$$

Following a similar procedure, we arrive at

$$\mathcal{L}_{\delta,\epsilon}^S \Pi^h \boldsymbol{u} = \frac{C_\alpha \mu}{m(\boldsymbol{x})} \mathcal{L}_{\delta,\epsilon}^B \Pi^h \boldsymbol{u} + \frac{C_\beta \mathrm{d}(\lambda - \mu)}{(m(\boldsymbol{x}))^2} \mathcal{G}_\delta^\epsilon \Pi^h (\mathcal{D}_\delta^\epsilon \Pi^h \boldsymbol{u}).$$

Let $S\left(\square \cap \Omega; \mathbb{R}^{\mathrm{d}}\right)$ be the space defined as

$$S\left(\square \cap \Omega; \mathbb{R}^{\mathrm{d}}\right) := \left\{ \boldsymbol{u} = \sum_{\boldsymbol{k} \in \mathbb{Z}^{\mathrm{d}}} \boldsymbol{u_k} \Psi_{\boldsymbol{k}} \,\middle|\, \boldsymbol{u_k} = \boldsymbol{0} \text{ for such } \boldsymbol{k} \text{ that } \boldsymbol{x_k} \notin (\square \cap \Omega) \right\}.$$

The RK collocation scheme of Eq. (9) is then written as follows. Find a function $\boldsymbol{u} \in S(\square \cap \Omega; \mathbb{R}^{\mathrm{d}})$, such that

$$-r_{\Omega}^{h} \mathcal{L}_{\delta}^{S} \boldsymbol{u} = r_{\Omega}^{h} \boldsymbol{f}. \tag{28}$$

Similarly, the RK collocation scheme of Eq. (20) is given as

$$-r_{\Omega}^{h} \mathcal{L}_{\delta,\epsilon}^{S} \boldsymbol{u} = r_{\Omega}^{h} \boldsymbol{f}, \tag{29}$$

for $\boldsymbol{u} \in S(\square \cap \Omega; \mathbb{R}^{\mathrm{d}})$. Here $\mathcal{L}_{\delta}^{S}\boldsymbol{u}$ and $\mathcal{L}_{\delta,\epsilon}^{S}\boldsymbol{u}$ represent, respectively,

$$\mathcal{L}_{\delta}^{S} \boldsymbol{u} = \frac{C_\alpha \mu}{m(\boldsymbol{x})} \mathcal{L}_{\delta}^{B} \boldsymbol{u} + \frac{C_\beta \mathrm{d}(\lambda - \mu)}{(m(\boldsymbol{x}))^2} \mathcal{G}_\delta \Pi^h (\mathcal{D}_\delta \boldsymbol{u}),$$

and

$$\mathcal{L}_{\delta,\epsilon}^{S} \boldsymbol{u} = \frac{C_\alpha \mu}{m(\boldsymbol{x})} \mathcal{L}_{\delta,\epsilon}^{B} \boldsymbol{u} + \frac{C_\beta \mathrm{d}(\lambda - \mu)}{(m(\boldsymbol{x}))^2} \mathcal{G}_\delta^\epsilon \Pi^h (\mathcal{D}_\delta^\epsilon \boldsymbol{u}).$$

The main contribution of this paper is to show the convergence analysis of the two collocation schemes Eqs. (28) and (29).

4. Convergence analysis of the RK collocation method

In this section, we show the convergence analysis of the RK collocation scheme Eq. (28), which is used in [14] without any analysis. The convergence study of Eq. (29) will be presented in Section 5. We note that a convergence proof of the RK collocation method for nonlocal diffusion problems is provided in [29], and the analysis is extended to the peridynamic Navier equation in this work. The main objective is to show that the solution of the numerical scheme converges to the nonlocal problem for a fixed δ as the grid size $h_{\max}$ vanishes, and to the correct local problem as δ and $h_{\max}$ both go to zero.

4.1. Stability

In this subsection, we show the stability of the RK collocation scheme Eq. (28). We first define a norm in the space of vector-valued sequences by

$$|(\boldsymbol{u}_{\boldsymbol{k}})_{\boldsymbol{k} \in \mathbb{Z}^{\mathrm{d}}}|_h := \|i^h(\boldsymbol{u}_{\boldsymbol{k}})\|_{L^2(\mathbb{R}^{\mathrm{d}};\, \mathbb{R}^{\mathrm{d}})}\ . \tag{30}$$

For a sequence $(\boldsymbol{u}_{\boldsymbol{k}})$ only defined for $\boldsymbol{k}$ being in a subset of $\mathbb{Z}^{\mathrm{d}}$, we can always extend $(\boldsymbol{u}_{\boldsymbol{k}})$ by zero to $\boldsymbol{k} \in \mathbb{Z}^{\mathrm{d}}$. Then without further explanation, $|(\boldsymbol{u}_{\boldsymbol{k}})|_h$ is always understood as (30) with zero extension. We present the stability result first and show the proof at the end of this subsection.

Theorem 4.1. *For any $\delta \in (0, \delta_0]$, there exists a constant $C > 0$ that depends on Ω and δ_0, such that for $\boldsymbol{u} \in S(\square \cap \Omega; \mathbb{R}^{\mathrm{d}})$,*

$$|r_{\Omega}^{h}(-\mathcal{L}_{\delta}^{S} \boldsymbol{u})|_h \geq C \|\boldsymbol{u}\|_{L^2(\mathbb{R}^{\mathrm{d}};\mathbb{R}^{\mathrm{d}})}.$$

To prove Theorem 4.1, we borrow the idea from [29,30] and compare the RK collocation scheme with the Galerkin scheme using Fourier analysis. Some intermediate results are required to facilitate the proof. We define an inner product in $l^2(\mathbb{Z}^{\mathrm{d}}; \mathbb{R}^{\mathrm{d}})$,

$$((\boldsymbol{u}_{\boldsymbol{k}}), (\boldsymbol{v}_{\boldsymbol{k}}))_{l^2} := \sum_{\boldsymbol{k} \in \mathbb{Z}^{\mathrm{d}}} u_{1,\boldsymbol{k}} v_{1,\boldsymbol{k}} + \cdots + \sum_{\boldsymbol{k} \in \mathbb{Z}^{\mathrm{d}}} u_{\mathrm{d},\boldsymbol{k}} v_{\mathrm{d},\boldsymbol{k}} = \sum_{j=1}^{\mathrm{d}} \sum_{\boldsymbol{k} \in \mathbb{Z}^{\mathrm{d}}} u_{j,\boldsymbol{k}} v_{j,\boldsymbol{k}}.$$

The Fourier series of a vector-valued sequence $(\boldsymbol{u}_{\boldsymbol{k}})$ is defined as

$$\widetilde{\boldsymbol{u}}(\boldsymbol{\xi}) = [\tilde{u}_1(\boldsymbol{\xi}), \ldots, \tilde{u}_{\mathrm{d}}(\boldsymbol{\xi})]^T$$

and the jth component of $\widetilde{\boldsymbol{u}}(\boldsymbol{\xi})$ is

$$\tilde{u}_j(\boldsymbol{\xi}) := \sum_{\boldsymbol{k} \in \mathbb{Z}^{\mathrm{d}}} e^{-i\boldsymbol{k}\cdot\boldsymbol{\xi}} u_{j,\boldsymbol{k}},$$

where

$$u_{j,\boldsymbol{k}} = (2\pi)^{-\mathrm{d}} \int_{\boldsymbol{Q}} e^{i\boldsymbol{k}\cdot\boldsymbol{\xi}} \tilde{u}_j(\boldsymbol{\xi}) d\boldsymbol{\xi},$$

for $\boldsymbol{Q} := (-\pi, \pi)^{\mathrm{d}}$.

We present the Fourier symbol of the peridynamic Navier operator $-\mathcal{L}_\delta^S$ in the next lemma. The Fourier transform of a function $\boldsymbol{u} \in L^2(\mathbb{R}^{\mathrm{d}}; \mathbb{R}^{\mathrm{d}})$ is defined by

$$\widehat{\boldsymbol{u}}(\boldsymbol{\xi}) := \int_{\mathbb{R}^{\mathrm{d}}} e^{-i\boldsymbol{x}\cdot\boldsymbol{\xi}} \boldsymbol{u}(\boldsymbol{x}) d\boldsymbol{x}.$$

The proof of the following lemma can be found in Appendix A.1.

Lemma 4.2. *The Fourier symbol of the peridynamic Navier operator $\mathcal{L}_\delta^S$ is given by*

$$-\widehat{\mathcal{L}_\delta^S \boldsymbol{u}}(\boldsymbol{\xi}) = \boldsymbol{M}_\delta^S(\boldsymbol{\xi}) \widehat{\boldsymbol{u}}(\boldsymbol{\xi}), \tag{31}$$

where the Fourier symbol $\boldsymbol{M}_\delta^S(\boldsymbol{\xi})$ is a $\mathrm{d} \times \mathrm{d}$ *matrix and consists of two parts,*

$$\boldsymbol{M}_\delta^S(\boldsymbol{\xi}) = \boldsymbol{M}_\delta^B(\boldsymbol{\xi}) + \boldsymbol{M}_\delta^D(\boldsymbol{\xi}), \tag{32}$$

where

$$\boldsymbol{M}_\delta^B(\boldsymbol{\xi}) = \frac{C_\mu}{\delta^2} p_1(\delta|\boldsymbol{\xi}|) \left(\boldsymbol{I}_{\mathrm{d}} - \vec{\boldsymbol{\xi}}\vec{\boldsymbol{\xi}}^T\right) + \frac{C_\mu}{\delta^2} q_1(\delta|\boldsymbol{\xi}|) \vec{\boldsymbol{\xi}}\vec{\boldsymbol{\xi}}^T, \tag{33}$$

and

$$\boldsymbol{M}_\delta^D(\boldsymbol{\xi}) = \frac{C_{\lambda,\mu}}{\delta^2} (b_1(\delta|\boldsymbol{\xi}|))^2 \vec{\boldsymbol{\xi}}\vec{\boldsymbol{\xi}}^T, \tag{34}$$

where $\boldsymbol{I}_{\mathrm{d}}$ is the d*-dimensional identity matrix, $\vec{\boldsymbol{\xi}} = \frac{\boldsymbol{\xi}}{|\boldsymbol{\xi}|}$ is the unit vector in the direction of $\boldsymbol{\xi}$, $C_\mu = C_\alpha \mu/\mathrm{d}$ and $C_{\lambda,\mu} = C_\beta(\lambda - \mu)$ are material dependent constants, the scalars $p_1(|\boldsymbol{\xi}|)$, $q_1(|\boldsymbol{\xi}|)$ and $b_1(|\boldsymbol{\xi}|)$ are given by*

$$p_1(|\boldsymbol{\xi}|) = \int_{B_1} \rho(|\boldsymbol{s}|) \frac{s_1^2}{|\boldsymbol{s}|^2} (1 - \cos(|\boldsymbol{\xi}| s_{\mathrm{d}})) d\boldsymbol{s}, \tag{35}$$

$$q_1(|\boldsymbol{\xi}|) = \int_{B_1} \rho(|\boldsymbol{s}|) \frac{s_{\mathrm{d}}^2}{|\boldsymbol{s}|^2} (1 - \cos(|\boldsymbol{\xi}| s_{\mathrm{d}})) d\boldsymbol{s}, \tag{36}$$

$$b_1(|\boldsymbol{\xi}|) = \int_{B_1} \rho(|\boldsymbol{s}|) s_{\mathrm{d}} \sin(|\boldsymbol{\xi}| s_{\mathrm{d}}) d\boldsymbol{s}. \tag{37}$$

If $C_{\lambda,\mu} \geq 0$, we can immediately see, from Eq. (32), that the Fourier symbol $\boldsymbol{M}_\delta^S(\boldsymbol{\xi})$ is positive definite as shown in the next lemma.

Lemma 4.3. *Assume $\lambda \geq \mu$, the Fourier symbol $\boldsymbol{M}_\delta^S(\boldsymbol{\xi})$ is positive definite for any $\boldsymbol{\xi} \neq \boldsymbol{0}$.*

Proof. By observation, $\boldsymbol{M}_\delta^S(\boldsymbol{\xi})$ is a real matrix. Moreover, from Eqs. (35) and (36) we know that

$$p_1(\delta|\boldsymbol{\xi}|), q_1(\delta|\boldsymbol{\xi}|) > 0, \qquad \text{for } \delta|\boldsymbol{\xi}| \neq 0.$$

Let $\boldsymbol{v}$ be a nonzero vector, then $|\boldsymbol{v}^T\vec{\boldsymbol{\xi}}| \leq |\boldsymbol{v}|$ since $|\vec{\boldsymbol{\xi}}| = 1$. Use Lemma 4.2 we have

$$\begin{aligned}
\delta^2 \boldsymbol{v}^T \boldsymbol{M}_\delta^S(\boldsymbol{\xi}) \boldsymbol{v} \geq\ & C_\mu p_1(\delta|\boldsymbol{\xi}|) \boldsymbol{v}^T \left(\boldsymbol{I}_{\mathrm{d}} - \vec{\boldsymbol{\xi}}\vec{\boldsymbol{\xi}}^T\right) \boldsymbol{v} \\
& + \left[C_\mu q_1(\delta|\boldsymbol{\xi}|) + C_{\lambda,\mu} (b_1(\delta|\boldsymbol{\xi}|))^2\right] \boldsymbol{v}^T \vec{\boldsymbol{\xi}}\vec{\boldsymbol{\xi}}^T \boldsymbol{v}, \\
=\ & C_\mu p_1(\delta|\boldsymbol{\xi}|) \left(|\boldsymbol{v}|^2 - |\boldsymbol{v}^T\vec{\boldsymbol{\xi}}|^2\right) \\
& + \left[C_\mu q_1(\delta|\boldsymbol{\xi}|) + C_{\lambda,\mu} (b_1(\delta|\boldsymbol{\xi}|))^2\right] |\boldsymbol{v}^T\vec{\boldsymbol{\xi}}|^2, \\
>\ & 0,
\end{aligned}$$

where we have used the assumption that $C_{\lambda,\mu} = \lambda - \mu \geq 0$. □

Remark 4.4. Notice that $\boldsymbol{M}_\delta^B(\boldsymbol{\xi})$ is a positive definite matrix for all nonzero $\boldsymbol{\xi}$. The assumption $\lambda \geq \mu$ ensures that $\boldsymbol{M}_\delta^D(\boldsymbol{\xi})$ is positive semidefinite, and simplifies the discussions of Fourier symbols for the discrete equations. We remind readers that the well-posedness of Eq. (9) proved in [10] is for general materials without this constraint.

The peridynamic Navier operator $\mathcal{L}_\delta^S$ defines two bilinear forms on $l^2(\mathbb{Z}^{\mathrm{d}}; \mathbb{R}^{\mathrm{d}})$:

$$\left(i^h(\boldsymbol{u}_{\boldsymbol{k}}), -\mathcal{L}_\delta^S i^h(\boldsymbol{v}_{\boldsymbol{k}})\right) = \sum_{\boldsymbol{k}, \boldsymbol{k}' \in \mathbb{Z}^{\mathrm{d}}} \left((\boldsymbol{u}_{\boldsymbol{k}} \Psi_{\boldsymbol{k}}), -\mathcal{L}_\delta^S(\boldsymbol{v}_{\boldsymbol{k}'} \Psi_{\boldsymbol{k}'})\right), \tag{38}$$

and

$$\left((\boldsymbol{u}_{\boldsymbol{k}}), -r^h \mathcal{L}_\delta^S i^h(\boldsymbol{v}_{\boldsymbol{k}})\right)_{l^2} = \prod_{j=1}^{\mathrm{d}} h_j \sum_{\boldsymbol{k}, \boldsymbol{k}' \in \mathbb{Z}^{\mathrm{d}}} (\boldsymbol{u}_{\boldsymbol{k}}) \cdot \left(-\mathcal{L}_\delta^S(\boldsymbol{v}_{\boldsymbol{k}'} \Psi_{\boldsymbol{k}'})\right)(\boldsymbol{x}_{\boldsymbol{k}}). \tag{39}$$

The inner product $(\cdot, \cdot)$ in Eq. (38) is the standard $L^2(\mathbb{R}^{\mathrm{d}}; \mathbb{R}^{\mathrm{d}})$ inner product defined as

$$(\boldsymbol{u}, \boldsymbol{v}) = \int_{\mathbb{R}^{\mathrm{d}}} \boldsymbol{u}(\boldsymbol{x}) \cdot \boldsymbol{v}(\boldsymbol{x}) d\boldsymbol{x} = \sum_{j=1}^{\mathrm{d}} \int_{\mathbb{R}^{\mathrm{d}}} u_j(\boldsymbol{x}) v_j(\boldsymbol{x}) d\boldsymbol{x} \quad \forall \boldsymbol{u}, \boldsymbol{v} \in L^2(\mathbb{R}^{\mathrm{d}}; \mathbb{R}^{\mathrm{d}}).$$

Hence, Eq. (38) defines a quadratic form corresponding to the Galerkin method, meanwhile, Eq. (39) corresponds to the collocation method. The following lemma compares the two quadratic forms Eqs. (38) and (39). The idea of the proof comes from [29, Lemma 4.2] but the derivations are much more involved. We provide the proof of Lemma 4.5 in Appendix A.2.

Lemma 4.5. *Let $\widetilde{\boldsymbol{u}}(\boldsymbol{\xi})$ and $\widetilde{\boldsymbol{v}}(\boldsymbol{\xi})$ be the Fourier series of the sequences $(\boldsymbol{u}_{\boldsymbol{k}}), (\boldsymbol{v}_{\boldsymbol{k}}) \in l^2(\mathbb{Z}^{\mathrm{d}}; \mathbb{R}^{\mathrm{d}})$ respectively. Then*

(i) $\left(i^h(\boldsymbol{u}_{\boldsymbol{k}}), -\mathcal{L}_\delta^S i^h(\boldsymbol{v}_{\boldsymbol{k}})\right) = (2\pi)^{-\mathrm{d}} \int_{\boldsymbol{Q}} \widetilde{\boldsymbol{u}}(\boldsymbol{\xi}) \cdot \boldsymbol{M}_G(\delta, \boldsymbol{h}, \boldsymbol{\xi}) \overline{\widetilde{\boldsymbol{v}}(\boldsymbol{\xi})} d\boldsymbol{\xi}$,

(ii) $\left((\boldsymbol{u}_{\boldsymbol{k}}), -r^h \mathcal{L}_\delta^S i^h(\boldsymbol{v}_{\boldsymbol{k}})\right)_{l^2} = (2\pi)^{-\mathrm{d}} \int_{\boldsymbol{Q}} \widetilde{\boldsymbol{u}}(\boldsymbol{\xi}) \cdot \boldsymbol{M}_C(\delta, \boldsymbol{h}, \boldsymbol{\xi}) \overline{\widetilde{\boldsymbol{v}}(\boldsymbol{\xi})} d\boldsymbol{\xi}$,

(iii) There exists a constant $C > 0$ independent of $\delta, \boldsymbol{h}$ and $\boldsymbol{\xi}$ such that $\boldsymbol{M}_C(\delta, \boldsymbol{h}, \boldsymbol{\xi}) - C\boldsymbol{M}_G(\delta, \boldsymbol{h}, \boldsymbol{\xi})$ is positive definite for any $\boldsymbol{\xi} \neq \boldsymbol{0}$,

where $\boldsymbol{M}_G$ and $\boldsymbol{M}_C$ are defined as

$$\begin{aligned}\boldsymbol{M}_G(\delta, \boldsymbol{h}, \boldsymbol{\xi}) = {} & 2^{8\mathrm{d}} \sum_{\boldsymbol{r} \in \mathbb{Z}^{\mathrm{d}}} \boldsymbol{M}_\delta^B\left((\boldsymbol{\xi} + 2\pi \boldsymbol{r}) \oslash \boldsymbol{h}\right) \prod_{j=1}^{\mathrm{d}} h_j \left(\frac{\sin(\xi_j/2)}{\xi_j + 2\pi r_j}\right)^8 \\ & + 2^{8\mathrm{d}+4} \sum_{\boldsymbol{r} \in \mathbb{Z}^{\mathrm{d}}} \boldsymbol{M}_\delta^D\left((\boldsymbol{\xi} + 2\pi \boldsymbol{r}) \oslash \boldsymbol{h}\right) \prod_{j=1}^{\mathrm{d}} h_j \left(\frac{\sin(\xi_j/2)}{\xi_j + 2\pi r_j}\right)^{12},\end{aligned} \tag{40}$$

$$\begin{aligned}\boldsymbol{M}_C(\delta, \boldsymbol{h}, \boldsymbol{\xi}) = {} & 2^{4\mathrm{d}} \sum_{\boldsymbol{r} \in \mathbb{Z}^{\mathrm{d}}} \boldsymbol{M}_\delta^B\left((\boldsymbol{\xi} + 2\pi \boldsymbol{r}) \oslash \boldsymbol{h}\right) \prod_{j=1}^{\mathrm{d}} h_j \left(\frac{\sin(\xi_j/2)}{\xi_j + 2\pi r_j}\right)^4 \\ & + 2^{4\mathrm{d}+4} \sum_{\boldsymbol{r} \in \mathbb{Z}^{\mathrm{d}}} \boldsymbol{M}_\delta^D\left((\boldsymbol{\xi} + 2\pi \boldsymbol{r}) \oslash \boldsymbol{h}\right) \prod_{j=1}^{\mathrm{d}} h_j \left(\frac{\sin(\xi_j/2)}{\xi_j + 2\pi r_j}\right)^8.\end{aligned} \tag{41}$$

Finally, we are ready to prove Theorem 4.1 using Lemma 4.5.

Proof of Theorem 4.1. The proof the theorem is similar to [29, Theorem 4.1]. For any sequence $(\boldsymbol{u}_{\boldsymbol{k}}) \in l^2(\mathbb{Z}^{\mathrm{d}}; \mathbb{R}^{\mathrm{d}})$, it is easy to see that the norm $|(\boldsymbol{u}_{\boldsymbol{k}})|_h$ defined in Eq. (30) is equivalent to $|(\boldsymbol{u}_{\boldsymbol{k}})|_{l^2}$. Then for $\boldsymbol{u} = i^h(\boldsymbol{u}_{\boldsymbol{k}}) \in S(\square \cap \Omega; \mathbb{R}^{\mathrm{d}})$, we have

$$\begin{aligned}|(\boldsymbol{u}_{\boldsymbol{k}})|_h \cdot |r_\Omega^h(-\mathcal{L}_\delta^S \boldsymbol{u})|_h &\geq C|((\boldsymbol{u}_{\boldsymbol{k}}), r_\Omega^h(-\mathcal{L}_\delta^S \boldsymbol{u}))_{l^2}|, \\ &= C|((\boldsymbol{u}_{\boldsymbol{k}}), r^h(-\mathcal{L}_\delta^S i^h(\boldsymbol{u}_{\boldsymbol{k}})))_{l^2}|,\end{aligned}$$

$$\geq C|(i^h(\boldsymbol{u_k}), (-\mathcal{L}_\delta^S i^h(\boldsymbol{u_k})))|,$$
$$\geq C\|\boldsymbol{u}\|^2_{L^2(\mathbb{R}^d;\,\mathbb{R}^d)}.$$

The first line comes from the Cauchy–Schwartz inequality and the third line from Lemma 4.5. The fourth line uses the stability result given in Theorem 2.1 since $\boldsymbol{u} = i^h(\boldsymbol{u_k}) \in S(\square \cap \Omega;\, \mathbb{R}^d) \subset \mathcal{S}_\delta$ and for a sufficiently large and fixed domain $\widetilde{\Omega} \supset \Omega$, we have $\boldsymbol{u}|_{\mathbb{R}^d\setminus\widetilde{\Omega}} = \boldsymbol{0}$. $\square$

4.2. Consistency

In this subsection, we show that the consistency error between the RK collocation scheme Eq. (28) and the nonlocal model Eq. (9) is uniformly bounded by $Ch^2_{\max}$ with a constant C independent of δ. Uniform consistency is the key to the asymptotic compatibility of a numerical method for nonlocal problems. If the RK support size is chosen carefully, the linear RK approximation has synchronized convergence property which is the major ingredient in the proof of uniform consistency. Indeed, it is shown in [29, Remark 3.2] and [36, Theorem 5.2] that the synchronized convergence property holds with RK support $\boldsymbol{a} = 2r_0\boldsymbol{h}$ ($r_0 \in \mathbb{N}$) for linear RK approximations. We skip the proof and present the result in the following lemma, and refer readers to [29,35–37] for more details. For the rest of the paper, we adopt the following notations for a vector-valued function $\boldsymbol{u} \in C^n(\mathbb{R}^d;\mathbb{R}^d)$,

$$|\boldsymbol{u}|_\infty = \sup_{1\leq j\leq d}\sup_{\boldsymbol{x}\in\mathbb{R}^d}|u_j(\boldsymbol{x})|, \text{ and}$$
$$|\boldsymbol{u}^{(l)}|_\infty = \sup_{1\leq j\leq d}\sup_{|\boldsymbol{\beta}|=l}\sup_{\boldsymbol{y}\in\mathbb{R}^d}|D^{\boldsymbol{\beta}}u_j(\boldsymbol{y})|, \quad 1\leq l\leq n.$$

Lemma 4.6 (*Synchronized Convergence*). *Let $u \in C^4(\mathbb{R}^d)$ be a scalar-valued function and $\Pi^h u$ be the RK interpolation of u with the shape function given by Eq. (25), then $\Pi^h u$ has synchronized convergence, namely*

$$\left|D^{\boldsymbol{\alpha}}(\Pi^h u - u)\right|_\infty \leq C|u^{(|\boldsymbol{\alpha}|+2)}|_\infty h^2_{\max}, \quad \text{for } |\boldsymbol{\alpha}| = 0, 1, 2,$$

where C is a generic constant independent of $h_{\max}$.

Next, we study the truncation error of the RK collocation method on the peridynamic Navier operator.

Lemma 4.7 (*Uniform Consistency*). *Assume $\boldsymbol{u} \in C^4(\mathbb{R}^d;\mathbb{R}^d)$, then*

$$|r^h\mathcal{L}_\delta^S\Pi^h\boldsymbol{u} - r^h\mathcal{L}_\delta^S\boldsymbol{u}|_h \leq Ch^2_{\max}|\boldsymbol{u}^{(4)}|_\infty,$$

where C is independent of $h_{\max}$ and δ.

Proof. We first define the interpolation error of $u_j(\boldsymbol{x})$, for $\boldsymbol{x} \in \mathbb{R}^d$, and $j = 1,\ldots,d$, as

$$E_j(\boldsymbol{x}) = \Pi^h u_j(\boldsymbol{x}) - u_j(\boldsymbol{x}),$$

then

$$\boldsymbol{E}(\boldsymbol{x}) = [E_1(\boldsymbol{x}),\ldots,E_d(\boldsymbol{x})]^T. \tag{42}$$

By restricting on the grid point $\boldsymbol{x_k}$, for $i = 1,\ldots,d$, the truncation error of $\mathcal{L}_\delta^B$ is given as

$$\left|\left[\mathcal{L}_\delta^B\left(\Pi^h\boldsymbol{u}-\boldsymbol{u}\right)\right]_i(\boldsymbol{x_k})\right| = \left|\left[\mathcal{L}_\delta^B\boldsymbol{E}\right]_i(\boldsymbol{x_k})\right|,$$

$$= \left|\sum_{j=1}^{d}\int_{B_\delta}\rho_\delta(|\boldsymbol{s}|)\frac{s_i s_j}{|\boldsymbol{s}|^2}\left(E_j(\boldsymbol{x_k}+\boldsymbol{s}) - E_j(\boldsymbol{x_k})\right)d\boldsymbol{s}\right|. \tag{43}$$

Next, using Lemma 4.6, we can bound the interpolation error by

$$\begin{aligned}|E_j(\boldsymbol{x_k}+\boldsymbol{s}) + E_j(\boldsymbol{x_k}-\boldsymbol{s}) - 2E_j(\boldsymbol{x_k})| &\leq C|\boldsymbol{s}|^2\max_{|\boldsymbol{\alpha}|=2}\left|D^{\boldsymbol{\alpha}}E_j(\boldsymbol{x})\right|_\infty,\\ &\leq C|\boldsymbol{s}|^2|u_j^{(4)}|_\infty h^2_{\max}.\end{aligned} \tag{44}$$

Combining Eqs. (43) and (44), we have

$$\begin{aligned}\left|[\mathcal{L}_\delta^B\left(\Pi^h \boldsymbol{u}-\boldsymbol{u}\right)(\boldsymbol{x}_{\boldsymbol{k}})]_i\right| &\leq C h_{\max}^2 \sum_{j=1}^{\mathrm{d}} |u_j^{(4)}|_\infty \int_{B_\delta} \rho_\delta(|\boldsymbol{s}|)|s_i||s_j|\, d\boldsymbol{s}, \\ &\leq C h_{\max}^2 \left|\boldsymbol{u}^{(4)}\right|_\infty,\end{aligned} \tag{45}$$

where we have used Eq. (3) and $C>0$ is a generic constant depending the dimension, d.

Next, we define the interpolation error of the nonlocal dilatation as

$$\begin{aligned}E_\theta &= \Pi^h \mathcal{D}_\delta \Pi^h \boldsymbol{u} - \mathcal{D}_\delta \boldsymbol{u}, \\ &= \Pi^h(\mathcal{D}_\delta \Pi^h \boldsymbol{u} - \mathcal{D}_\delta \boldsymbol{u}) + \Pi^h \mathcal{D}_\delta \boldsymbol{u} - \mathcal{D}_\delta \boldsymbol{u}, \\ &= \Pi^h \mathcal{D}_\delta \boldsymbol{E} + (\Pi^h \theta - \theta),\end{aligned} \tag{46}$$

where we have used the definition of the nonlocal dilatation Eq. (6). There are two RK interpolation projectors (Π^h) in the first line of Eq. (46) because we apply RK interpolation to $\boldsymbol{u}$ and θ, then back-substitute θ to get a pure displacement form. The nonlocal gradient operator acting on E_θ can be bounded by

$$\begin{aligned}|[\mathcal{G}_\delta E_\theta(\boldsymbol{x}_{\boldsymbol{k}})]_i| &= \left|\int_{B_\delta} \rho_\delta(|\boldsymbol{t}|) t_i \left(E_\theta(\boldsymbol{x}_{\boldsymbol{k}}+\boldsymbol{t}) - E_\theta(\boldsymbol{x}_{\boldsymbol{k}})\right) d\boldsymbol{t}\right|, \\ &\leq \max_{|\boldsymbol{\beta}|=1} \left|D^{\boldsymbol{\beta}} E_\theta\right|_\infty \int_{B_\delta} \rho_\delta(|\boldsymbol{t}|)|t_i||\boldsymbol{t}|\, d\boldsymbol{t}, \\ &\leq C \max_{|\boldsymbol{\beta}|=1} \left|D^{\boldsymbol{\beta}} E_\theta\right|_\infty, \\ &\leq C \max_{|\boldsymbol{\beta}|=1} \left|D^{\boldsymbol{\beta}} \Pi^h \mathcal{D}_\delta \boldsymbol{E}\right|_\infty + C \max_{|\boldsymbol{\beta}|=1} \left|D^{\boldsymbol{\beta}} (\Pi^h \theta - \theta)\right|_\infty,\end{aligned} \tag{47}$$

for $i=1,\ldots,\mathrm{d}$. We can bound the first term in the last line of Eq. (47) by

$$\begin{aligned}\max_{|\boldsymbol{\beta}|=1} \left|D^{\boldsymbol{\beta}} \Pi^h \mathcal{D}_\delta \boldsymbol{E}\right|_\infty &= \max_{|\boldsymbol{\beta}|=1} \left|\sum_{j=1}^{\mathrm{d}} D^{\boldsymbol{\beta}} \Pi^h \int_{B_\delta} \rho_\delta(|\boldsymbol{s}|) s_j \left(E_j(\boldsymbol{x}+\boldsymbol{s}) - E_j(\boldsymbol{x})\right) d\boldsymbol{s}\right|_\infty, \\ &\leq \sum_{j=1}^{\mathrm{d}} \int_{B_\delta} \rho_\delta(|\boldsymbol{s}|)|s_j||\boldsymbol{s}| d\boldsymbol{s} \max_{|\boldsymbol{\alpha}|=|\boldsymbol{\beta}|=1} \left|D^{\boldsymbol{\beta}} \Pi^h D^{\boldsymbol{\alpha}} E_j(\boldsymbol{x})\right|_\infty, \\ &\leq C h_{\max}^2 \left|\boldsymbol{u}^{(4)}\right|_\infty,\end{aligned} \tag{48}$$

where the derivation of the second line to the last can be obtained by similar expansion of [37, eq.(36)] and the results of [43, Lemma 4.1] together with Lemma 4.6. Next, we have the bound of the second term in the last line of Eq. (47) as

$$\max_{|\boldsymbol{\beta}|=1} \left|D^{\boldsymbol{\beta}} (\Pi^h \theta - \theta)\right|_\infty \leq C \left|\theta^{(3)}\right|_\infty h_{\max}^2, \tag{49}$$

and $\left|\theta^{(3)}\right|_\infty$ is bounded by

$$\begin{aligned}\left|\theta^{(3)}\right|_\infty &= \frac{\mathrm{d}}{m(\boldsymbol{x})} \max_{|\boldsymbol{\beta}|=3} \left|\sum_{j=1}^{\mathrm{d}} D^{\boldsymbol{\beta}} \int_{B_\delta} \rho_\delta(|\boldsymbol{s}|) s_j \left(u_j(\boldsymbol{x}+\boldsymbol{s}) - u_j(\boldsymbol{x})\right) d\boldsymbol{s}\right|_\infty, \\ &\leq C \sum_{j=1}^{\mathrm{d}} \int_{B_\delta} \rho_\delta(|\boldsymbol{s}|)|s_j||\boldsymbol{s}| d\boldsymbol{s} \max_{|\boldsymbol{\alpha}|=4} \left|D^{\boldsymbol{\alpha}} u_j(\boldsymbol{x})\right|_\infty, \\ &\leq C \left|\boldsymbol{u}^{(4)}\right|_\infty.\end{aligned} \tag{50}$$

By collecting Eqs. (47)–(50), we can bound the truncation error of the composition of the nonlocal gradient and divergence operators by

$$\left|[(\mathcal{G}_\delta \Pi^h \mathcal{D}_\delta \Pi^h \boldsymbol{u} - \mathcal{G}_\delta \mathcal{D}_\delta \boldsymbol{u})(\boldsymbol{x}_{\boldsymbol{k}})]_i\right| \leq C h_{\max}^2 \left|\boldsymbol{u}^{(4)}\right|_\infty. \tag{51}$$

Finally, the proof is finished by combining Eqs. (45) and (51). □

4.3. Convergence

We conclude this section by showing the convergence results of the RK collocation method. The RK collocation scheme converges to the nonlocal solution as grid size $h_{\max}$ goes to zero for a fixed δ and to the corresponding local limit as δ and $h_{\max}$ both vanish. Combining the stability Theorem 4.1 and the consistency Lemma 4.7 of the RK collocation method, we can immediately show the convergence to the nonlocal solution. We present the following theorem without proof as it follows the procedure similarly as in [29, Theorem 4.7].

Theorem 4.8 (*Uniform Convergence to Nonlocal Solution*)**.** *For a fixed $\delta \in (0, \delta_0]$, assume the nonlocal exact solution $\boldsymbol{u}^\delta$ is sufficiently smooth, i.e., $\boldsymbol{u}^\delta \in C^4\left(\overline{\Omega_{2\delta}};\, \mathbb{R}^{\mathrm{d}}\right)$. Moreover, assume $|\boldsymbol{u}^{\delta(4)}|_\infty$ is uniformly bounded for every δ. Let $\boldsymbol{u}^{\delta,h}$ be the numerical solution of the collocation scheme Eq. (28), then,*

$$\|\boldsymbol{u}^\delta - \boldsymbol{u}^{\delta,h}\|_{L^2(\Omega;\,\mathbb{R}^{\mathrm{d}})} \leq C h_{\max}^2,$$

where C is independent of $h_{\max}$ and δ.

Before showing that the convergence of the RK collocation scheme to the local limit is independent of δ, we need the bound of truncation error between the collocation scheme and the local limit of the peridynamic Navier model.

Lemma 4.9 (*Asymptotic Consistency I*)**.** *Assume $\boldsymbol{u} \in C^4(\mathbb{R}^{\mathrm{d}};\, \mathbb{R}^{\mathrm{d}})$, then*

$$|r^h \mathcal{L}_\delta^S \Pi^h \boldsymbol{u} - r^h \mathcal{L}_0^S \boldsymbol{u}|_h \leq C |\boldsymbol{u}^{(4)}|_\infty (h_{\max}^2 + \delta^2),$$

where C is independent of $h_{\max}$ and δ.

Proof. From Lemma 4.7 and the continuous property of the nonlocal operators, we have

$$\begin{aligned} \left|r^h \mathcal{L}_\delta^S \Pi^h \boldsymbol{u} - r^h \mathcal{L}_0^S \boldsymbol{u}\right|_h &\leq \left|r^h \mathcal{L}_\delta^S \Pi^h \boldsymbol{u} - r^h \mathcal{L}_\delta^S \boldsymbol{u}\right|_h + \left|r^h \mathcal{L}_\delta^S \boldsymbol{u} - r^h \mathcal{L}_0^S \boldsymbol{u}\right|_h, \\ &\leq C \left|\boldsymbol{u}^{(4)}\right|_\infty (h_{\max}^2 + \delta^2). \quad \square \end{aligned}$$

Combining Theorem 4.1 and Lemma 4.9, we have the uniform convergence (asymptotic compatibility) to the local limit. We leave out the proof of the next theorem for conciseness because it is similar to the proof of Theorem 4.8.

Theorem 4.10 (*Asymptotic Compatibility*)**.** *Assume the local exact solution $\boldsymbol{u}^0$ is sufficiently smooth, i.e., $\boldsymbol{u}^0 \in C^4(\overline{\Omega_{2\delta}};\, \mathbb{R}^{\mathrm{d}})$. For any $\delta \in (0, \delta_0]$, $\boldsymbol{u}^{\delta,h}$ is the numerical solution of the collocation scheme Eq. (28), then,*

$$\|\boldsymbol{u}^0 - \boldsymbol{u}^{\delta,h}\|_{L^2(\Omega;\,\mathbb{R}^{\mathrm{d}})} \leq C(h_{\max}^2 + \delta^2).$$

5. Convergence analysis of the RK collocation on the quasi-discrete peridynamic Navier equation

In practice, accurate evaluation of the integral in nonlocal models is computationally prohibitive especially if the nonlocal kernel is singular. This motivates us to use the quasi-discrete nonlocal models as introduced in Section 2.2. It is practical to couple δ with grid size $h_{\max}$ because this results in a banded linear system. In this section, we assume $\delta = M_0 h_{\max}$ where $M_0 > 0$. As $h_{\max}$ goes to zero, so does δ, and the quasi-discrete nonlocal operator converges to its local limit. We provide convergence analysis of the collocation scheme Eq. (29) to its local limit.

5.1. Stability

We start with the stability of the collocation scheme Eq. (29).

Theorem 5.1. *For any $\delta \in (0, \delta_0]$, there exists a generic constant $C > 0$ which depends on Ω, δ_0 and M_0, such that for $\boldsymbol{u} \in S(\square \cap \Omega; \mathbb{R}^{\mathrm{d}})$,*

$$|r_\Omega^h(-\mathcal{L}_{\delta,\epsilon}^S \boldsymbol{u})|_h \geq C \|\boldsymbol{u}\|_{L^2(\mathbb{R}^{\mathrm{d}};\,\mathbb{R}^{\mathrm{d}})}.$$

To prove Theorem 5.1, we need the Fourier symbol of the quasi-discrete peridynamic Navier operator $\mathcal{L}^S_{\delta,\epsilon}$, shown in Lemma 5.2. We present the lemma without proof because the proof follows similarly as Lemma 4.2 using the fact that the quadrature points are symmetric and the quadrature weights are positive, see Eq. (13).

Lemma 5.2. *The Fourier symbol of the quasi-discrete peridynamic Navier operator $\mathcal{L}^S_{\delta,\epsilon}$ is given by*

$$-\widehat{\mathcal{L}^S_{\delta,\epsilon}\boldsymbol{u}}(\boldsymbol{\xi}) = \boldsymbol{M}^S_{\delta,\epsilon}(\boldsymbol{\xi})\widehat{\boldsymbol{u}}(\boldsymbol{\xi}), \tag{52}$$

where the Fourier symbol $\boldsymbol{M}^S_{\delta,\epsilon}(\boldsymbol{\xi})$ is a $\mathrm{d}\times\mathrm{d}$ matrix and can be written as

$$\boldsymbol{M}^S_{\delta,\epsilon}(\boldsymbol{\xi}) = \boldsymbol{M}^B_{\delta,\epsilon}(\boldsymbol{\xi}) + \boldsymbol{M}^D_{\delta,\epsilon}(\boldsymbol{\xi}), \tag{53}$$

where

$$\boldsymbol{M}^B_{\delta,\epsilon}(\boldsymbol{\xi}) = \frac{C_\mu}{\delta^2} p_1^{\epsilon 1}(\delta|\boldsymbol{\xi}|)\left(\boldsymbol{I}_\mathrm{d} - \vec{\boldsymbol{\xi}}\vec{\boldsymbol{\xi}}^T\right) + \frac{C_\mu}{\delta^2} q_1^{\epsilon 1}(\delta|\boldsymbol{\xi}|)\vec{\boldsymbol{\xi}}\vec{\boldsymbol{\xi}}^T, \tag{54}$$

and

$$\boldsymbol{M}^D_{\delta,\epsilon}(\boldsymbol{\xi}) = \frac{C_{\lambda,\mu}}{\delta^2}\left(b_1^{\epsilon 1}(\delta|\boldsymbol{\xi}|)\right)^2 \vec{\boldsymbol{\xi}}\vec{\boldsymbol{\xi}}^T, \tag{55}$$

where the scalars $p_1^{\epsilon 1}(|\boldsymbol{\xi}|)$, $q_1^{\epsilon 1}(|\boldsymbol{\xi}|)$ and $b_1^{\epsilon 1}(|\boldsymbol{\xi}|)$ are given as follows

$$p_1^{\epsilon 1}(|\boldsymbol{\xi}|) = \sum_{\boldsymbol{s}\in B_1^{\epsilon 1}} \omega(|\boldsymbol{s}|)\rho(|\boldsymbol{s}|)\frac{s_1^2}{|\boldsymbol{s}|^2}(1-\cos(|\boldsymbol{\xi}|s_\mathrm{d})), \tag{56}$$

$$q_1^{\epsilon 1}(|\boldsymbol{\xi}|) = \sum_{\boldsymbol{s}\in B_1^{\epsilon 1}} \omega(|\boldsymbol{s}|)\rho(|\boldsymbol{s}|)\frac{s_\mathrm{d}^2}{|\boldsymbol{s}|^2}(1-\cos(|\boldsymbol{\xi}|s_\mathrm{d})), \tag{57}$$

$$b_1^{\epsilon 1}(|\boldsymbol{\xi}|) = \sum_{\boldsymbol{s}\in B_1^{\epsilon 1}} \omega(|\boldsymbol{s}|)\rho(|\boldsymbol{s}|)s_\mathrm{d}\sin(|\boldsymbol{\xi}|s_\mathrm{d}). \tag{58}$$

From Lemma 5.2, we have the Fourier representation of the collocation scheme on the quasi-discrete peridynamic Navier operator as follows.

Lemma 5.3. *Let $\widetilde{\boldsymbol{u}}(\boldsymbol{\xi})$ and $\widetilde{\boldsymbol{v}}(\boldsymbol{\xi})$ be the Fourier series of the sequences $(\boldsymbol{u}_{\boldsymbol{k}}), (\boldsymbol{v}_{\boldsymbol{k}}) \in l^2(\mathbb{Z}^\mathrm{d};\mathbb{R}^\mathrm{d})$ respectively. Then*

$$((\boldsymbol{u}_{\boldsymbol{k}}), -r^h\mathcal{L}^S_{\delta,\epsilon}i^h(\boldsymbol{v}_{\boldsymbol{k}}))_{l^2} = (2\pi)^{-\mathrm{d}}\int_{\boldsymbol{Q}} \widetilde{\boldsymbol{u}}(\boldsymbol{\xi})\cdot \boldsymbol{M}^\epsilon_C(\delta,\boldsymbol{h},\boldsymbol{\xi})\overline{\widetilde{\boldsymbol{v}}(\boldsymbol{\xi})}d\boldsymbol{\xi}\,, \tag{59}$$

where $\boldsymbol{M}^\epsilon_C$ is defined as

$$\begin{aligned}\boldsymbol{M}^\epsilon_C(\delta,\boldsymbol{h},\boldsymbol{\xi}) = {} & 2^{4\mathrm{d}}\sum_{\boldsymbol{r}\in\mathbb{Z}^\mathrm{d}} \boldsymbol{M}^B_{\delta,\epsilon}((\boldsymbol{\xi}+2\pi\boldsymbol{r})\oslash\boldsymbol{h})\prod_{j=1}^{\mathrm{d}} h_j\left(\frac{\sin(\xi_j/2)}{\xi_j+2\pi r_j}\right)^4 \\ & + 2^{4\mathrm{d}+4}\sum_{\boldsymbol{r}\in\mathbb{Z}^\mathrm{d}} \boldsymbol{M}^D_{\delta,\epsilon}((\boldsymbol{\xi}+2\pi\boldsymbol{r})\oslash\boldsymbol{h})\prod_{j=1}^{\mathrm{d}} h_j\left(\frac{\sin(\xi_j/2)}{\xi_j+2\pi r_j}\right)^8.\end{aligned} \tag{60}$$

Moreover, there exists $C>0$, independent of δ and $\boldsymbol{h}$ such that,

$$\boldsymbol{M}^\epsilon_C(\delta,\boldsymbol{h},\boldsymbol{\xi}) - C\boldsymbol{M}_C(\delta,\boldsymbol{h},\boldsymbol{\xi}) \tag{61}$$

is positive definite for any $\boldsymbol{\xi}\neq\boldsymbol{0}$.

Proof. The derivation of Eq. (60) is similar to Eq. (41), we can simply replace $\boldsymbol{M}^S_\delta(\boldsymbol{\xi}+2\pi\boldsymbol{r})$ with $\boldsymbol{M}^S_{\delta,\epsilon}(\boldsymbol{\xi}+2\pi\boldsymbol{r})$. The challenge is to show that Eq. (61) is positive definite.

Following similar arguments in the proof of [29, lemma 6.2] to obtain [29, eq.(6.8)], we have for $\boldsymbol{\xi}\in\boldsymbol{Q}$,

$$p_1^{\epsilon 1}(\delta|\boldsymbol{\xi}\oslash\boldsymbol{h}|)\prod_{j=1}^{\mathrm{d}} h_j\left(\frac{\sin(\xi_j/2)}{\xi_j+2\pi r_j}\right)^4 \geq C_p^{\epsilon 1}|\boldsymbol{\xi}|^2\prod_{j=1}^{\mathrm{d}} h_j\,. \tag{62}$$

Similarly, we can obtain

$$q_1^{\epsilon_1}(\delta|\boldsymbol{\xi}\oslash\boldsymbol{h}|)\prod_{j=1}^{\mathrm{d}}h_j\left(\frac{\sin(\xi_j/2)}{\xi_j+2\pi r_j}\right)^4\geq C_q^{\epsilon_1}|\boldsymbol{\xi}|^2\prod_{j=1}^{\mathrm{d}}h_j, \tag{63}$$

where $C_q^{\epsilon_1}>0$ is a generic constant. Combining Eqs. (62) and (63), we have the following bound, for $\boldsymbol{\xi}\in\boldsymbol{Q}$,

$$\begin{aligned}\boldsymbol{M}_C^{\epsilon}(\delta,\boldsymbol{h},\boldsymbol{\xi})&\geq C_\mu\left(\frac{|\boldsymbol{\xi}|}{\delta}\right)^2\left\{C_p^{\epsilon_1}\left(\boldsymbol{I}_{\mathrm{d}}-\vec{\boldsymbol{\xi}}_{\boldsymbol{h}}\vec{\boldsymbol{\xi}}_{\boldsymbol{h}}^T\right)+C_q^{\epsilon_1}\vec{\boldsymbol{\xi}}_{\boldsymbol{h}}\vec{\boldsymbol{\xi}}_{\boldsymbol{h}}^T\right\}\prod_{j=1}^{\mathrm{d}}h_j\\&\geq\min\{C_p^{\epsilon_1},C_q^{\epsilon_1}\}C_\mu\left(\frac{|\boldsymbol{\xi}|}{\delta}\right)^2\prod_{j=1}^{\mathrm{d}}h_j\,\boldsymbol{I}_{\mathrm{d}}\geq C\left(\frac{|\boldsymbol{\xi}|}{\delta}\right)^2\prod_{j=1}^{\mathrm{d}}h_j\,\boldsymbol{I}_{\mathrm{d}},\end{aligned} \tag{64}$$

where $\boldsymbol{\xi}_{\boldsymbol{h}}=\boldsymbol{\xi}\oslash\boldsymbol{h}$ and we have ignored the terms for $\boldsymbol{r}\neq\boldsymbol{0}$ because they are non-negative and positive definite.

Next, we use the fact that

$$1-\cos(x)\leq x^2\ \text{and}\ \sin(x)\leq x,\quad\text{for } x\geq 0,$$

to obtain, for any $\boldsymbol{r}\in\mathbb{Z}^{\mathrm{d}}$,

$$p_1(\delta|(\boldsymbol{\xi}+2\pi\boldsymbol{r})\oslash\boldsymbol{h}|)\leq\left(\frac{\delta|\boldsymbol{\xi}+2\pi\boldsymbol{r}|}{h_{\max}}\right)^2\int_{B_1}\rho(|\boldsymbol{s}|)\frac{s_1^2s_{\mathrm{d}}^2}{|\boldsymbol{s}|^2}d\boldsymbol{s}\leq C|\boldsymbol{\xi}+2\pi\boldsymbol{r}|^2,$$

and

$$q_1(\delta|(\boldsymbol{\xi}+2\pi\boldsymbol{r})\oslash\boldsymbol{h}|)\leq C|\boldsymbol{\xi}+2\pi\boldsymbol{r}|^2,\quad b_1(\delta|(\boldsymbol{\xi}+2\pi\boldsymbol{r})\oslash\boldsymbol{h}|)\leq C|\boldsymbol{\xi}+2\pi\boldsymbol{r}|,$$

where we have used Eq. (3). Hence we obtain

$$\begin{aligned}&p_1(\delta|(\boldsymbol{\xi}+2\pi\boldsymbol{r})\oslash\boldsymbol{h}|)\prod_{j=1}^{\mathrm{d}}h_j\left(\frac{\sin(\xi_j/2)}{\xi_j+2\pi r_j}\right)^4\\&\leq C|(\boldsymbol{\xi}+2\pi\boldsymbol{r})|^2\left(\frac{\sin(\boldsymbol{\xi}/2)}{\boldsymbol{\xi}+2\pi\boldsymbol{r}}\right)^4\prod_{j=1}^{\mathrm{d}}h_j\leq C_p\frac{|\boldsymbol{\xi}|^2}{|\boldsymbol{\xi}_{\boldsymbol{r}}|^2}\prod_{j=1}^{\mathrm{d}}h_j,\end{aligned} \tag{65}$$

where $\boldsymbol{\xi}_{\boldsymbol{r}}=\boldsymbol{\xi}+2\pi\boldsymbol{r}$ and C_p is a generic constant. Similarly,

$$q_1(\delta|(\boldsymbol{\xi}+2\pi\boldsymbol{r})\oslash\boldsymbol{h}|)\prod_{j=1}^{\mathrm{d}}h_j\left(\frac{\sin(\xi_j/2)}{\xi_j+2\pi r_j}\right)^4\leq C_q\frac{|\boldsymbol{\xi}|^2}{|\boldsymbol{\xi}_{\boldsymbol{r}}|^2}\prod_{j=1}^{\mathrm{d}}h_j \tag{66}$$

and

$$[b_1(\delta|(\boldsymbol{\xi}+2\pi\boldsymbol{r})\oslash\boldsymbol{h}|)]^2\prod_{j=1}^{\mathrm{d}}h_j\left(\frac{\sin(\xi_j/2)}{\xi_j+2\pi r_j}\right)^8\leq C_b\frac{|\boldsymbol{\xi}|^2}{|\boldsymbol{\xi}_{\boldsymbol{r}}|^2}\prod_{j=1}^{\mathrm{d}}h_j, \tag{67}$$

where $C_q, C_b>0$. By gathering Eqs. (65)–(67), we have

$$\begin{aligned}&\boldsymbol{M}_C(\delta,\boldsymbol{h},\boldsymbol{\xi})\\&\leq\left(\frac{|\boldsymbol{\xi}|}{\delta}\right)^2\sum_{\boldsymbol{r}\in\mathbb{Z}^{\mathrm{d}}}\frac{C_pC_\mu\left(\boldsymbol{I}_{\mathrm{d}}-\vec{\boldsymbol{\xi}}_{\boldsymbol{h},\boldsymbol{r}}\vec{\boldsymbol{\xi}}_{\boldsymbol{h},\boldsymbol{r}}^T\right)+C_qC_\mu\vec{\boldsymbol{\xi}}_{\boldsymbol{h},\boldsymbol{r}}\vec{\boldsymbol{\xi}}_{\boldsymbol{h},\boldsymbol{r}}^T+C_bC_{\lambda,\mu}\vec{\boldsymbol{\xi}}_{\boldsymbol{h},\boldsymbol{r}}\vec{\boldsymbol{\xi}}_{\boldsymbol{h},\boldsymbol{r}}^T}{|\boldsymbol{\xi}_{\boldsymbol{r}}|^2}\prod_{j=1}^{\mathrm{d}}h_j,\\&\leq C\left(\frac{|\boldsymbol{\xi}|}{\delta}\right)^2\prod_{j=1}^{\mathrm{d}}h_j\,\boldsymbol{I}_{\mathrm{d}},\end{aligned} \tag{68}$$

where $\boldsymbol{\xi}_{\boldsymbol{h},\boldsymbol{r}}=(\boldsymbol{\xi}+2\pi\boldsymbol{r})\oslash\boldsymbol{h}$.

Finally, Eq. (61) is shown by combining Eqs. (64) and (68). □

Proof of Theorem 5.1. By applying Lemma 5.3, the proof follows similarly to the proof of Theorem 4.1. □

5.2. Consistency

In this subsection, we establish the consistency of collocation scheme Eq. (29) the and its local limit as δ and $h_{\max}$ both go to zero. The following lemma shows the truncation error between $\mathcal{L}^S_\delta$ and $\mathcal{L}^S_{\delta,\epsilon}$ with the ratio ϵ/δ being fixed.

Lemma 5.4. *Assume $\boldsymbol{u} \in C^4(\mathbb{R}^{\mathrm{d}};\mathbb{R}^{\mathrm{d}})$, then for $i = 1,\ldots,\mathrm{d}$,*

$$\left|\left[\mathcal{L}^S_{\delta,\epsilon}\boldsymbol{u} - \mathcal{L}^S_\delta \boldsymbol{u}\right]_i\right| \le C\delta^2 \left|\boldsymbol{u}^{(4)}\right|_\infty .$$

Proof. Using Taylor's theorem, for $\boldsymbol{x} \in \mathbb{R}^{\mathrm{d}}$, $j = 1,\ldots,\mathrm{d}$, and $\boldsymbol{s} \in B_\delta$ we have

$$u_j(\boldsymbol{x}+\boldsymbol{s}) - u_j(\boldsymbol{x}) = \sum_{|\boldsymbol{\alpha}|=1,2} \boldsymbol{s}^{\boldsymbol{\alpha}} \frac{D^{\boldsymbol{\alpha}} u_j(\boldsymbol{x})}{\boldsymbol{\alpha}!} + \sum_{|\boldsymbol{\beta}|=3} \boldsymbol{s}^{\boldsymbol{\beta}} \frac{R_j^{\boldsymbol{\beta},+}(\boldsymbol{x})}{\boldsymbol{\beta}!}, \tag{69}$$

and

$$\begin{aligned} u_j(\boldsymbol{x}+\boldsymbol{s}) &+ u_j(\boldsymbol{x}-\boldsymbol{s}) - 2u_j(\boldsymbol{x}) \\ &= 2\sum_{|\boldsymbol{\alpha}|=2} \boldsymbol{s}^{\boldsymbol{\alpha}} \frac{D^{\boldsymbol{\alpha}} u_j(\boldsymbol{x})}{\boldsymbol{\alpha}!} + \sum_{|\boldsymbol{\beta}|=4} \boldsymbol{s}^{\boldsymbol{\beta}} \frac{R_j^{\boldsymbol{\beta},+}(\boldsymbol{x}) + R_j^{\boldsymbol{\beta},-}(\boldsymbol{x})}{\boldsymbol{\beta}!}, \end{aligned} \tag{70}$$

where $R_j^{\boldsymbol{\beta},\pm}(\boldsymbol{x})$ is given by

$$R_j^{\boldsymbol{\beta},\pm}(\boldsymbol{x}) = |\boldsymbol{\beta}| \int_0^1 (1-\tau)^{|\boldsymbol{\beta}|-1} \left|D^{\boldsymbol{\beta}}\left(u_j(\boldsymbol{x} \pm \tau \boldsymbol{s})\right)\right| d\tau . \tag{71}$$

Notice that $|R_j^{\boldsymbol{\beta},\pm}(\boldsymbol{x})| \le C|u_j^{(|\boldsymbol{\beta}|)}|_\infty$. For simplicity of presentation, we now write $R_j^{\boldsymbol{\beta}}(\boldsymbol{x}) := R_j^{\boldsymbol{\beta},+}(\boldsymbol{x}) + R_j^{\boldsymbol{\beta},-}(\boldsymbol{x})$. First, we study the truncation error between $\mathcal{L}^B_\delta \boldsymbol{u}$ and $\mathcal{L}^B_{\delta,\epsilon}\boldsymbol{u}$, for $i = 1,\ldots,\mathrm{d}$,

$$\begin{aligned} &\left|[\mathcal{L}^B_{\delta,\epsilon}\boldsymbol{u}(\boldsymbol{x}) - \mathcal{L}^B_\delta \boldsymbol{u}(\boldsymbol{x})]_i\right| \\ &= \Bigg| \sum_{j=1}^{\mathrm{d}} \sum_{|\boldsymbol{\alpha}|=2} \frac{D^{\boldsymbol{\alpha}} u_j(\boldsymbol{x})}{\boldsymbol{\alpha}!} \left(\sum_{\boldsymbol{s}\in B^\epsilon_\delta} \omega_\delta(|\boldsymbol{s}|)\rho_\delta(|\boldsymbol{s}|) \frac{s_i s_j}{|\boldsymbol{s}|^2} \boldsymbol{s}^{\boldsymbol{\alpha}} - \int_{B_\delta} \rho_\delta(|\boldsymbol{s}|) \frac{s_i s_j}{|\boldsymbol{s}|^2} \boldsymbol{s}^{\boldsymbol{\alpha}} d\boldsymbol{s} \right) \\ &+ \sum_{|\boldsymbol{\beta}|=4} \frac{1}{2\boldsymbol{\beta}!} \left(\sum_{\boldsymbol{s}\in B^\epsilon_\delta} \omega_\delta(|\boldsymbol{s}|)\rho_\delta(|\boldsymbol{s}|) \frac{s_i s_j}{|\boldsymbol{s}|^2} \boldsymbol{s}^{\boldsymbol{\beta}} R_j^{\boldsymbol{\beta}}(\boldsymbol{x}) - \int_{B_\delta} \rho_\delta(|\boldsymbol{s}|) \frac{s_i s_j}{|\boldsymbol{s}|^2} \boldsymbol{s}^{\boldsymbol{\beta}} R_j^{\boldsymbol{\beta}}(\boldsymbol{x}) d\boldsymbol{s} \right) \Bigg| \\ &\le 0 + \left|\boldsymbol{u}^{(4)}\right|_\infty \sum_{j=1}^{\mathrm{d}} \sum_{|\boldsymbol{\beta}|=4} \left(\sum_{\boldsymbol{s}\in B^\epsilon_\delta} \omega_\delta(|\boldsymbol{s}|)\rho_\delta(|\boldsymbol{s}|) \frac{|s_i s_j|}{|\boldsymbol{s}|^2} |\boldsymbol{s}|^{\boldsymbol{\beta}} + \int_{B_\delta} \rho_\delta(|\boldsymbol{s}|) \frac{|s_i s_j|}{|\boldsymbol{s}|^2} |\boldsymbol{s}|^{\boldsymbol{\beta}} d\boldsymbol{s} \right), \\ &\le C\delta^2 \left|\boldsymbol{u}^{(4)}\right|_\infty , \end{aligned} \tag{72}$$

where we have used Eqs. (4), (14), (23) and (70).

Next, via Eq. (69), the quasi-discrete nonlocal divergence operator $\mathcal{D}^\epsilon_\delta$ acting on $\boldsymbol{u}$ can be written as

$$\begin{aligned} \mathcal{D}^\epsilon_\delta \boldsymbol{u}(\boldsymbol{x}) &= \sum_{j=1}^{\mathrm{d}} \sum_{|\boldsymbol{\alpha}|=1,2} \frac{D^{\boldsymbol{\alpha}} u_j(\boldsymbol{x})}{\boldsymbol{\alpha}!} \sum_{\boldsymbol{s}\in B^\epsilon_\delta} \omega_\delta(|\boldsymbol{s}|)\rho_\delta(|\boldsymbol{s}|) s_j \boldsymbol{s}^{\boldsymbol{\alpha}} \\ &\quad + \sum_{j=1}^{\mathrm{d}} \sum_{|\boldsymbol{\beta}|=3} \frac{1}{\boldsymbol{\beta}!} \sum_{\boldsymbol{s}\in B^\epsilon_\delta} \omega_\delta(|\boldsymbol{s}|)\rho_\delta(|\boldsymbol{s}|) s_j \boldsymbol{s}^{\boldsymbol{\beta}} R_j^{\boldsymbol{\beta},+}(\boldsymbol{x}), \\ &= \sum_{j=1}^{\mathrm{d}} \frac{\partial u_j}{\partial x_j}(\boldsymbol{x}) + \sum_{j=1}^{\mathrm{d}} \sum_{|\boldsymbol{\beta}|=3} \frac{1}{\boldsymbol{\beta}!} \sum_{\boldsymbol{s}\in B^\epsilon_\delta} \omega_\delta(|\boldsymbol{s}|)\rho_\delta(|\boldsymbol{s}|) s_j \boldsymbol{s}^{\boldsymbol{\beta}} R_j^{\boldsymbol{\beta},+}(\boldsymbol{x}), \end{aligned} \tag{73}$$

where we have used Eq. (12) as well as the symmetry of the quadrature points. We immediately have a similar result for $\mathcal{D}_\delta$,

$$\mathcal{D}_\delta \boldsymbol{u}(\boldsymbol{x}) = \sum_{j=1}^{\mathrm{d}} \frac{\partial u_j}{\partial x_j}(\boldsymbol{x}) + \sum_{j=1}^{\mathrm{d}} \sum_{|\boldsymbol{\beta}|=3} \frac{1}{\boldsymbol{\beta}!} \int_{B_\delta} \rho_\delta(|\boldsymbol{s}|) s_j \boldsymbol{s}^{\boldsymbol{\beta}} R_j^{\boldsymbol{\beta},+}(\boldsymbol{x}) d\boldsymbol{s}. \tag{74}$$

Then, the truncation error between $\mathcal{G}_\delta^\epsilon \mathcal{D}_\delta^\epsilon \boldsymbol{u}$ and $\mathcal{G}_\delta \mathcal{D}_\delta \boldsymbol{u}$ is given by

$$\begin{aligned}
&\left|[\mathcal{G}_\delta^\epsilon \mathcal{D}_\delta^\epsilon \boldsymbol{u} - \mathcal{G}_\delta \mathcal{D}_\delta \boldsymbol{u}]_i(\boldsymbol{x})\right| \\
&= \Bigg| \sum_{j=1}^{\mathrm{d}} \sum_{|\boldsymbol{\alpha}|=1,2} \frac{D^{\boldsymbol{\alpha}}(\partial u_j/\partial x_j)(\boldsymbol{x})}{\boldsymbol{\alpha}!} \left(\sum_{\boldsymbol{t}\in B_\delta^\epsilon} \omega_\delta(|\boldsymbol{t}|)\rho_\delta(|\boldsymbol{t}|) t_i \boldsymbol{t}^{\boldsymbol{\alpha}} - \int_{B_\delta} \rho_\delta(|\boldsymbol{t}|) t_i \boldsymbol{t}^{\boldsymbol{\alpha}} d\boldsymbol{t} \right) \\
&+ \sum_{j=1}^{\mathrm{d}} \sum_{|\boldsymbol{\gamma}|=3} \frac{1}{\boldsymbol{\gamma}!} \left(\sum_{\boldsymbol{t}\in B_\delta^\epsilon} \omega_\delta(|\boldsymbol{t}|)\rho_\delta(|\boldsymbol{t}|) t_i \boldsymbol{t}^{\boldsymbol{\gamma}} \tilde{R}_j^{\boldsymbol{\gamma},+}(\boldsymbol{x}) - \int_{B_\delta} \rho_\delta(|\boldsymbol{t}|) t_i \boldsymbol{t}^{\boldsymbol{\gamma}} \tilde{R}_j^{\boldsymbol{\gamma},+}(\boldsymbol{x}) d\boldsymbol{t} \right) \\
&+ \sum_{j=1}^{\mathrm{d}} \sum_{|\boldsymbol{\beta}|=3} \frac{1}{\boldsymbol{\beta}!} \sum_{\boldsymbol{t}\in B_\delta^\epsilon} \omega_\delta(|\boldsymbol{t}|)\rho_\delta(|\boldsymbol{t}|) t_i \sum_{\boldsymbol{s}\in B_\delta^\epsilon} \omega_\delta(|\boldsymbol{s}|)\rho_\delta(|\boldsymbol{s}|) s_j \boldsymbol{s}^{\boldsymbol{\beta}} \left(R_j^{\boldsymbol{\beta},+}(\boldsymbol{x}+\boldsymbol{t}) - R_j^{\boldsymbol{\beta},+}(\boldsymbol{x}) \right) \\
&- \sum_{j=1}^{\mathrm{d}} \sum_{|\boldsymbol{\beta}|=3} \frac{1}{\boldsymbol{\beta}!} \int_{B_\delta} \rho_\delta(|\boldsymbol{t}|) t_i \int_{B_\delta} \rho_\delta(|\boldsymbol{s}|) s_j \boldsymbol{s}^{\boldsymbol{\beta}} \left(R_j^{\boldsymbol{\beta},+}(\boldsymbol{x}+\boldsymbol{t}) - R_j^{\boldsymbol{\beta},+}(\boldsymbol{x}) \right) d\boldsymbol{s} d\boldsymbol{t} \Bigg|, \\
&\le 0 + C \left(\sum_{j=1}^{\mathrm{d}} \sum_{|\boldsymbol{\gamma}|=3} \frac{\left|\boldsymbol{u}^{(4)}\right|_\infty}{\boldsymbol{\gamma}!} \sum_{\boldsymbol{t}\in B_\delta^\epsilon} \omega_\delta(|\boldsymbol{t}|)\rho_\delta(|\boldsymbol{t}|) |t_i| |\boldsymbol{t}^{\boldsymbol{\gamma}}| + \int_{B_\delta} \rho_\delta(|\boldsymbol{t}|) |t_i| |\boldsymbol{t}^{\boldsymbol{\gamma}}| d\boldsymbol{t} \right) \\
&\quad + \sum_{j=1}^{\mathrm{d}} \sum_{|\boldsymbol{\beta}|=3} \frac{\left|\boldsymbol{u}^{(4)}\right|_\infty}{\boldsymbol{\beta}!} \sum_{\boldsymbol{t}\in B_\delta^\epsilon} \omega_\delta(|\boldsymbol{t}|)\rho_\delta(|\boldsymbol{t}|) |t_i| |\boldsymbol{t}| \sum_{\boldsymbol{s}\in B_\delta^\epsilon} \omega_\delta(|\boldsymbol{s}|)\rho_\delta(|\boldsymbol{s}|) |s_j| \left|\boldsymbol{s}^{\boldsymbol{\beta}}\right| \\
&\quad + \sum_{j=1}^{\mathrm{d}} \sum_{|\boldsymbol{\beta}|=3} \frac{\left|\boldsymbol{u}^{(4)}\right|_\infty}{\boldsymbol{\beta}!} \int_{B_\delta} \omega_\delta(|\boldsymbol{t}|)\rho_\delta(|\boldsymbol{t}|) |t_i| |\boldsymbol{t}| d\boldsymbol{t} \int_{B_\delta} \omega_\delta(|\boldsymbol{s}|)\rho_\delta(|\boldsymbol{s}|) |s_j| \left|\boldsymbol{s}^{\boldsymbol{\beta}}\right| d\boldsymbol{s} \\
&\le C\delta^2 \left|\boldsymbol{u}^{(4)}\right|_\infty .
\end{aligned} \tag{75}$$

where $\tilde{R}_j^{\boldsymbol{\gamma},+}$ is the remainder by expanding $\partial u_j/\partial x_j$ similarly as Eq. (69). Notice that in Eq. (75) we have used Eqs. (73) and (74), and the fact that

$$\left| R_j^{\boldsymbol{\beta},+}(\boldsymbol{x}+\boldsymbol{t}) - R_j^{\boldsymbol{\beta},+}(\boldsymbol{x}) \right| \le C \left| u_j^{(|\boldsymbol{\beta}|+1)} \right|_\infty |\boldsymbol{t}|,$$

which comes from the definition Eq. (71).

Eqs. (72) and (75) together complete the proof. □

Lemma 5.4 shows that with the number of quadrature points inside the horizon being fixed, the error between $\mathcal{L}_\delta^S \boldsymbol{u}$ and $\mathcal{L}_{\delta,\epsilon}^S \boldsymbol{u}$ is of the order $O(\delta^2)$. So to reduce the error between them, one needs to reduce the horizon size δ. We also note that [29, Remark 5.2] shows if δ is fixed, the error between the quasi-discrete and continuous nonlocal diffusion operator is bounded by $O(\epsilon^2)$ and similar results could also be derived for the peridynamic Navier operator. However, this is to say that if nonlocal limit (δ being fixed) is of interest, then one has to increase the number of quadrature points in the horizon ($\epsilon \to 0$) for the quasi-discrete nonlocal operator to approximate the continuous nonlocal operator. In this work, since our concern is to reduce the computational cost by using only a few quadrature points (see numerical examples in Section 6), we only discuss the case that the number of quadrature points is fixed in the horizon.

Now, we present the discrete model error between the quasi-discrete nonlocal peridynamic Navier equation and its local limit.

Lemma 5.5 (*Asymptotic Consistency II*). *Assume $\boldsymbol{u} \in C^4(\mathbb{R}^{\mathrm{d}}; \mathbb{R}^{\mathrm{d}})$, then*

$$|r_\Omega^h \mathcal{L}_{\delta,\epsilon}^S \Pi^h \boldsymbol{u} - r_\Omega^h \mathcal{L}_0^S \boldsymbol{u}^0|_h \le C \left|\boldsymbol{u}^{(4)}\right|_\infty (h_{\max}^2 + \delta^2).$$

Proof. In order to prove this lemma, we need the following intermediate result

$$\left|r^h \mathcal{L}^S_{\delta,\epsilon} \Pi^h \boldsymbol{u} - r^h \mathcal{L}^S_{\delta,\epsilon} \boldsymbol{u}\right|_h \le C h^2_{\max} \left|\boldsymbol{u}^{(4)}\right|_\infty . \tag{76}$$

The proof of Eq. (76) is similar to Lemma 4.7, following the replacement of the nonlocal operators with their quasi-discrete counterparts.

By collecting Eq. (76) and Lemma 5.4, the discrete model error of collocation scheme Eq. (29) is given as

$$\begin{aligned}\left|r^h \mathcal{L}^S_{\delta,\epsilon} \Pi^h \boldsymbol{u} - r^h \mathcal{L}^S_{0} \boldsymbol{u}\right|_h &\le \left|r^h \mathcal{L}^S_{\delta,\epsilon} \Pi^h \boldsymbol{u} - r^h \mathcal{L}^S_{\delta,\epsilon} \boldsymbol{u}\right|_h + \left|r^h \mathcal{L}^S_{\delta,\epsilon} \boldsymbol{u} - r^h \mathcal{L}^S_{\delta} \boldsymbol{u}\right|_h \\ &\quad + \left|r^h \mathcal{L}^S_{\delta} \boldsymbol{u} - r^h \mathcal{L}^S_{0} \boldsymbol{u}\right|_h , \\ &\le C \left|\boldsymbol{u}^{(4)}\right|_\infty (h^2_{\max} + \delta^2 + \delta^2). \quad \square\end{aligned}$$

5.3. Convergence

Combining Theorem 5.1 and Lemma 5.5, we follow similar procedure as the proof Theorem 4.8 and show that the numerical solution of Eq. (29) converges to its local limit.

Theorem 5.6. *Assume the local exact solution $\boldsymbol{u}^0$ is sufficiently smooth, i.e., $\boldsymbol{u}^0 \in C^4(\overline{\Omega_{\delta_0}}; \mathbb{R}^{\mathrm{d}})$. For any $\delta \in (0, \delta_0]$, let $\boldsymbol{u}^{\delta,\epsilon,h}$ be the numerical solution of the collocation scheme Eq. (29) and fix the ratio between δ and $h_{\max}$. Then,*

$$\|\boldsymbol{u}^0 - \boldsymbol{u}^{\delta,\epsilon,h}\|_{L^2(\Omega;\mathbb{R}^{\mathrm{d}})} \le C(h^2_{\max} + \delta^2).$$

6. Numerical example

In this section, we validate the convergence analysis in the previous sections by considering a numerical example in two dimension. We let the discretization parameter be $\boldsymbol{h} = (h_1, h_2)$ where $h_1 = 2h_2$, then $h_{\max} = h_1$. Choosing the manufactured solution $\boldsymbol{u}(x_1, x_2) = [x_1^2(1-x_1)^2 + x_2^2(1-x_2)^2, 0]^T$, we obtain the right-hand side of Eqs. (9) and (11) as

$$\boldsymbol{f}_\delta(\boldsymbol{x}) = \boldsymbol{f}_0(\boldsymbol{x}) - \left[\frac{18\lambda}{5}\delta^2,\ 0\right]^T$$

where

$$\boldsymbol{f}_0(\boldsymbol{x}) = -\left[2\lambda(1 - 6x_1 + 6x_2^2) + 6\mu(1 - 4x_1 + 4x_1^2 - 2x_2 + 2x_2^2),\ 0\right]^T .$$

We impose the corresponding values of $\boldsymbol{u}(\boldsymbol{x})$ on $\Omega_{\mathcal{I}_2}$ such that the exact value to the local limit matches on $\partial\Omega$. The nonlocal kernel is chosen as $\rho_\delta(|\boldsymbol{s}|) = \frac{3}{2\pi\delta^3|\boldsymbol{s}|}$, and let $\Omega = (0, 1)^2$, $E = 1$ and $\nu = 0.4$. Therefore, the Lamé parameters $\lambda = E\nu/((1+\nu)(1-2\nu))$ and $\mu = E/(2(1+\nu))$ satisfy the assumption in Lemma 4.3. In the example with a fixed δ, we solve the following peridynamic Navier equation

$$\begin{cases}-\mathcal{L}^S_\delta \boldsymbol{u}(\boldsymbol{x}) = \boldsymbol{f}_\delta(\boldsymbol{x}), & \boldsymbol{x} \in \Omega, \\ \quad \boldsymbol{u}(\boldsymbol{x}) = \left[x_1^2(1-x_1^2) + x_2^2(1-x_2^2), 0\right]^T , & \boldsymbol{x} \in \Omega_{\mathcal{I}_2} .\end{cases} \tag{77}$$

When testing the convergence rate as δ and $h_{\max}$ both go to zero, we solve another nonlocal problem

$$\begin{cases}-\mathcal{L}^S_\delta \boldsymbol{u}(\boldsymbol{x}) = \boldsymbol{f}_0(\boldsymbol{x}), & \boldsymbol{x} \in \Omega, \\ \quad \boldsymbol{u}(\boldsymbol{x}) = \left[x_1^2(1-x_1^2) + x_2^2(1-x_2^2), 0\right]^T , & \boldsymbol{x} \in \Omega_{\mathcal{I}_2},\end{cases} \tag{78}$$

which converges to the local limit

$$\begin{cases}-\mathcal{L}^S_0 \boldsymbol{u}(\boldsymbol{x}) = \boldsymbol{f}_0(\boldsymbol{x}), & \boldsymbol{x} \in \Omega, \\ \quad \boldsymbol{u}(\boldsymbol{x}) = \left[x_1^2(1-x_1^2) + x_2^2(1-x_2^2), 0\right]^T , & \boldsymbol{x} \in \partial\Omega.\end{cases}$$

We apply the two collocation schemes as Eqs. (28) and (29) and investigate their convergence properties.

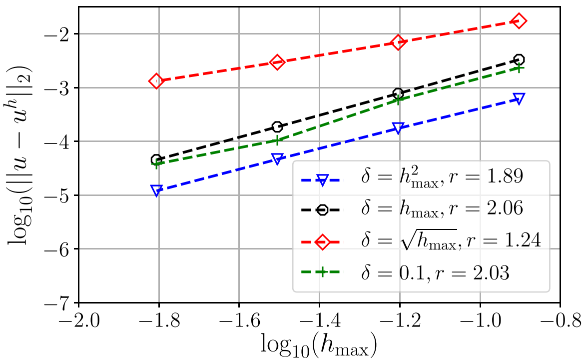

Fig. 2. Convergence profiles using the RK collocation method.

6.1. RK collocation

We first use the scheme as described in Eq. (28) to solve Eq. (77) for a fixed δ and study the convergence property to the nonlocal limit. Then we investigate the convergence of the numerical solution to the local limit by solving Eq. (78) and letting δ go to zero. Integration schemes play a significant role in the convergence profile as shown in [14]. We apply Gauss integration scheme proposed in [14], and use around 1000 quadrature points in the horizon of each collocation point so that the integration error is negligible.

Fig. 2 shows the convergence profiles. When δ is fixed, the numerical solution converges to the nonlocal solution at a second-order convergence rate with error measured in L^2 norm. Then we couple δ with $h_{\max}$ by letting both δ and $h_{\max}$ go to zero but at different rates, numerical solutions converge to the local limit. Second-order convergence rates are observed when δ goes to zero faster ($\delta = h_{\max}^2$) and at the same rate as $h_{\max}$ ($\delta = h_{\max}$). We only obtain a first-order convergence rate when $\delta = \sqrt{h_{\max}}$. The convergence behavior agrees with Theorems 4.8 and 4.10 and the numerical examples have verified that the RK collocation method is an AC scheme.

6.2. RK collocation on quasi-discrete peridynamic Navier equation

To avoid the need of using high-order Gauss quadrature rules, we have reformulated the peridynamic Navier equation in Section 2.2, using the quasi-discrete nonlocal operators. It is also more practical to couple the horizon with grid size as $\delta = M_0 h_{\max}$ because this leads to banded linear systems amenable to traditional preconditioning techniques. Now, we use the RK collocation method on the quasi-discrete peridynamic Navier equation as discussed in Eq. (29) to solve Eq. (78) and study the convergence to the local limit as δ and $h_{\max}$ approach to 0 at the same rate. In this experiment, we let $\delta = 3\epsilon$, thus there are 29 integration points in the horizon of each collocation point, see Fig. 1. Fig. 3 presents the convergence profiles and second-order convergence rates are observed. The numerical findings agree with our analysis in Theorem 5.6 and verify that the RK collocation on quasi-discrete peridynamic Navier equation converges to the correct local limit. When the local limit is of our interest, the computational cost of using the quasi-discrete nonlocal operators is significantly reduced, compared to Section 6.1.

7. Conclusion

In this work, we have designed and analyzed a linear RK collocation method for the peridynamic Navier equation. We first apply linear RK approximation to both the displacements and dilatation, and then back-substitute dilatation into the equation and solve it in a pure displacement form. Numerical solutions of the method converge to both the nonlocal solution when δ is fixed and its local limit when δ vanishes; convergence analysis of this scheme is presented in the case of Cartesian grids with varying resolution in each dimension. Because the standard Galerkin scheme has been proven to be stable, the key idea of analyzing the stability of the collocation scheme is to establish a relationship between the two schemes. In order to show stability of numerical schemes, we also assume the material parameters satisfy $\lambda \geq \mu$ to simplify the discussion, and our analysis is applicable for materials that satisfy this constraint.

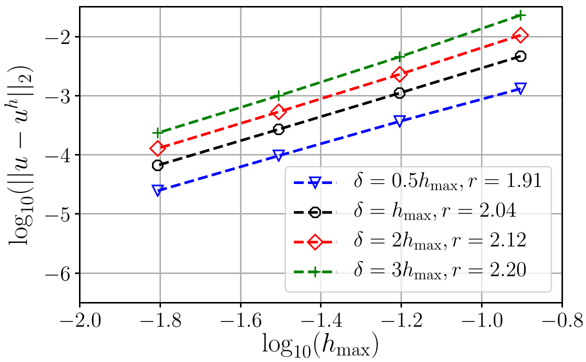

Fig. 3. Convergence profiles using the RK collocation on quasi-discrete peridynamic Navier equation.

In addition, we formulate the quasi-discrete version of the peridynamics Navier equation using quasi-discrete nonlocal operators first proposed in [29] for nonlocal diffusion problems. The key is to replace the integral with a finite summation of symmetric quadrature points in the horizon with carefully designated quadrature weights satisfying polynomial reproducing conditions for a given nonlocal (even singular) kernel. Under the assumption that the quadrature points are symmetrically distributed and that the quadrature weights are positive, we show the convergence of the RK collocation method on the quasi-discrete peridynamics Navier equation. The discrete solution of the RK collocation method applied to the quasi-discrete peridynamic Navier equation converges to the correct local limit.

Compared with previous work [29] on nonlocal diffusion problems, this work is new in the following aspects. First, the Fourier analysis is extended to the peridynamic Navier system of equations. The Fourier symbol of the peridynamic Navier operator is a matrix and consists of two parts, while the Fourier symbol of the nonlocal diffusion is a scalar; more involved derivations are done for the Fourier representations of the collocation schemes of the peridynamic Navier operator and its quasi-discrete counterpart. Second, we construct the quasi-discrete peridynamic Navier operator with appropriate quadrature weights. A reformulation of the bounded second-order moment condition is required to guarantee consistency.

In addition, numerical examples in two dimension are conducted to complement our mathematical analysis and the same order of convergence is observed as our theoretical result has predicted. That is, for the RK collocation method, the numerical solution converges to the nonlocal solution for a fixed δ at the order $O(h_{\max}^2)$ and to the corresponding local solution at the order $O(\delta^2 + h_{\max}^2)$; for the RK collocation method on the quasi-discrete peridynamic Navier equation, the numerical solution converges to the correct local limit at second order when the ratio $\delta/h_{\max}$ is fixed.

Finally, we remark that there are some interesting topics remain to be addressed in the future. We only consider fixed $\delta/h_{\max}$ for the quasi-discrete peridynamic Navier equation in this work, it is worthwhile to study the case for uncoupled δ and $h_{\max}$. For classical (local) linear elasticity, FEM solution obtained from the pure displacement form often deteriorates and becomes unstable when ν is close to 0.5. For the peridynamic Navier equation, however, numerical results in [45] show that the meshfree discretization converges to the local limit with a second-order convergence rate even for $\nu = 0.495$. It is then interesting to explore the numerical analysis for the nearly impressible materials. Moreover, our analysis is limited on rectilinear Cartesian grids but rigorous analysis on a more general grid, such as quasi-uniform grid, should also be studied in the near future.

Declaration of competing interest

The authors declare that they have no known competing financial interests or personal relationships that could have appeared to influence the work reported in this paper.

Acknowledgments

The research of Yu Leng and John T. Foster is supported in part by the AFOSR MURI Center for Material Failure Prediction through Peridynamics (AFOSR Grant Number FA9550-14-1-0073) and the SNL:LDRD academic alliance program. The work of Xiaochuan Tian is supported in part by NSF grant DMS-1819233. Nathaniel Trask also acknowledges funding under the DOE ASCR PhILMS center (Grant Number DE-SC001924) and the Laboratory Directed Research and Development program at Sandia National Laboratories. Sandia National Laboratories is a multi-program laboratory managed and operated by National Technology and Engineering Solutions of Sandia, LLC., a wholly owned subsidiary of Honeywell International, Inc., for the U.S. Department of Energy's National Nuclear Security Administration under contract DE-NA-0003525.

The Oden Institute is acknowledged for its support. The authors also thank Leszek Demkowicz, Qiang Du and Xiao Xu for helpful discussions on the subject.

Appendix

A.1. Proof of Lemma 4.2

We need to calculate the Fourier symbol of the nonlocal operators first.

Lemma A.1. *The Fourier symbol of the operators $\mathcal{L}_\delta^B, \mathcal{G}_\delta, \mathcal{D}_\delta$ are given by*

$$-\widehat{\mathcal{L}_\delta^B \boldsymbol{u}}(\boldsymbol{\xi}) = \boldsymbol{M}_\delta^B(\boldsymbol{\xi})\widehat{\boldsymbol{u}}(\boldsymbol{\xi}), \tag{A.1}$$

$$\widehat{\mathcal{G}_\delta \theta}(\boldsymbol{\xi}) = i\boldsymbol{b}_\delta(\boldsymbol{\xi})\widehat{\theta}(\boldsymbol{\xi}), \tag{A.2}$$

$$\widehat{\mathcal{D}_\delta \boldsymbol{u}}(\boldsymbol{\xi}) = i\boldsymbol{b}_\delta^T(\boldsymbol{\xi})\widehat{\boldsymbol{u}}(\boldsymbol{\xi}), \tag{A.3}$$

where $\boldsymbol{M}_\delta^B(\boldsymbol{\xi})$ is a $\mathrm{d}\times\mathrm{d}$ *matrix and $\boldsymbol{b}_\delta(\boldsymbol{\xi})$ is a vector. They are expressed as*

$$\begin{aligned}\boldsymbol{M}_\delta^B(\boldsymbol{\xi}) &= \int_{B_\delta} \rho_\delta(|\boldsymbol{s}|)\frac{\boldsymbol{s}\otimes\boldsymbol{s}}{|\boldsymbol{s}|^2}(1-\cos(\boldsymbol{s}\cdot\boldsymbol{\xi}))d\boldsymbol{s},\\ &= p_\delta(|\boldsymbol{\xi}|)\left(\boldsymbol{I}_\mathrm{d} - \vec{\boldsymbol{\xi}}\vec{\boldsymbol{\xi}}^{\,T}\right) + q_\delta(|\boldsymbol{\xi}|)\vec{\boldsymbol{\xi}}\vec{\boldsymbol{\xi}}^{\,T},\end{aligned} \tag{A.4}$$

and

$$\boldsymbol{b}_\delta(\boldsymbol{\xi}) = \int_{B_\delta} \rho_\delta(|\boldsymbol{s}|)\boldsymbol{s}\sin(\boldsymbol{s}\cdot\boldsymbol{\xi})d\boldsymbol{s} = b_\delta(|\boldsymbol{\xi}|)\vec{\boldsymbol{\xi}}\,, \tag{A.5}$$

where $\vec{\boldsymbol{\xi}} = \frac{\boldsymbol{\xi}}{|\boldsymbol{\xi}|}$ is the unit vector in the direction of $\boldsymbol{\xi}$ and the scalars $p_\delta(|\boldsymbol{\xi}|), q_\delta(|\boldsymbol{\xi}|)$ and $b_\delta(|\boldsymbol{\xi}|)$ are given by

$$p_\delta(|\boldsymbol{\xi}|) = \int_{B_\delta} \rho_\delta(|\boldsymbol{s}|)\frac{s_1^2}{|\boldsymbol{s}|^2}(1-\cos(|\boldsymbol{\xi}|s_\mathrm{d}))d\boldsymbol{s}, \tag{A.6}$$

$$q_\delta(|\boldsymbol{\xi}|) = \int_{B_\delta} \rho_\delta(|\boldsymbol{s}|)\frac{s_\mathrm{d}^2}{|\boldsymbol{s}|^2}(1-\cos(|\boldsymbol{\xi}|s_\mathrm{d}))d\boldsymbol{s}, \tag{A.7}$$

$$b_\delta(|\boldsymbol{\xi}|) = \int_{B_\delta} \rho_\delta(|\boldsymbol{s}|)s_\mathrm{d}\sin(|\boldsymbol{\xi}|s_\mathrm{d})d\boldsymbol{s}. \tag{A.8}$$

Proof. The derivations of Eqs. (A.1)–(A.3) follow directly from the definition of these nonlocal operators. The derivation of $\boldsymbol{b}_\delta(\boldsymbol{\xi})$ can be found in [40], and we follow the same strategy to show $\boldsymbol{M}_\delta^B(\boldsymbol{\xi})$,

$$\begin{aligned}-\widehat{\mathcal{L}_\delta^B \boldsymbol{u}}(\boldsymbol{\xi}) &= -\int_{\mathbb{R}^3} e^{-i\boldsymbol{x}\cdot\boldsymbol{\xi}}\int_{B_\delta}\rho_\delta(|\boldsymbol{s}|)\frac{\boldsymbol{s}\otimes\boldsymbol{s}}{|\boldsymbol{s}|^2}(\boldsymbol{u}(\boldsymbol{x}+\boldsymbol{s})-\boldsymbol{u}(\boldsymbol{x}))d\boldsymbol{s}d\boldsymbol{x},\\ &= -\int_{B_\delta}\int_{\mathbb{R}^3}\rho_\delta(|\boldsymbol{s}|)\frac{\boldsymbol{s}\otimes\boldsymbol{s}}{|\boldsymbol{s}|^2}(\boldsymbol{u}(\boldsymbol{x}+\boldsymbol{s})-\boldsymbol{u}(\boldsymbol{x}))e^{-i\boldsymbol{x}\cdot\boldsymbol{\xi}}d\boldsymbol{x}d\boldsymbol{s},\\ &= \int_{B_\delta}\rho_\delta(|\boldsymbol{s}|)\frac{\boldsymbol{s}\otimes\boldsymbol{s}}{|\boldsymbol{s}|^2}(1-e^{i\boldsymbol{s}\cdot\boldsymbol{\xi}})\widehat{\boldsymbol{u}}(\boldsymbol{\xi})d\boldsymbol{s},\\ &= \boldsymbol{M}_\delta^B(\boldsymbol{\xi})\widehat{\boldsymbol{u}}(\boldsymbol{\xi}),\end{aligned}$$

where $\boldsymbol{M}_\delta^B(\boldsymbol{\xi})$ is given by the first line of Eq. (A.4) and we have used the symmetry of the nonlocal kernel $\rho_\delta(|\boldsymbol{s}|)$.

We proceed to show the second line of Eq. (A.4) only for d = 3 because the case d = 2 is similar. For any orthogonal matrix $\boldsymbol{\mathcal{R}}$, we have

$$\boldsymbol{M}_\delta^B(\boldsymbol{\xi}) = \boldsymbol{\mathcal{R}}^T \boldsymbol{M}_\delta^B(\boldsymbol{\mathcal{R}}\boldsymbol{\xi})\boldsymbol{\mathcal{R}}.$$

We let $\boldsymbol{\mathcal{R}}$ be the orthogonal matrix which rotates $\boldsymbol{\xi}$ to be aligned with $\boldsymbol{e}$, ($\boldsymbol{e} = (0, 0, 1)^T$), i.e.,

$$\boldsymbol{\mathcal{R}}\boldsymbol{\xi} = |\boldsymbol{\xi}|\boldsymbol{e}.$$

Then $\boldsymbol{\mathcal{R}}\boldsymbol{\xi} \cdot \boldsymbol{s} = |\boldsymbol{\xi}|s_3$ and we have

$$\boldsymbol{M}_\delta^B(\boldsymbol{\xi}) = \int_{B_\delta} \rho_\delta(|\boldsymbol{s}|)\frac{1-\cos(|\boldsymbol{\xi}|s_3)}{|\boldsymbol{s}|^2}\boldsymbol{\mathcal{R}}^T\boldsymbol{s}(\boldsymbol{\mathcal{R}}^T\boldsymbol{s})^T d\boldsymbol{s},$$

$\boldsymbol{\mathcal{R}}$ is the rotation matrix that rotates $\boldsymbol{\xi}$ by an angle of

$$\arccos\left(\boldsymbol{e}\cdot\frac{\boldsymbol{\xi}}{|\boldsymbol{\xi}|}\right) = \arccos\left(\frac{\xi_3}{|\boldsymbol{\xi}|}\right),$$

around the axis in the direction of

$$\frac{\boldsymbol{\xi}\times\boldsymbol{e}}{|\boldsymbol{\xi}\times\boldsymbol{e}|} = \frac{1}{\sqrt{\xi_1^2+\xi_2^2}}(\xi_2, -\xi_1, 0).$$

$\boldsymbol{\mathcal{R}}$ can be explicitly constructed as

$$\boldsymbol{\mathcal{R}} = \begin{bmatrix} \frac{\xi_3}{|\boldsymbol{\xi}|} + \frac{\xi_2^2}{\xi_1^2+\xi_2^2}\left(1-\frac{\xi_3}{|\boldsymbol{\xi}|}\right) & \frac{-\xi_1\xi_2}{\xi_1^2+\xi_2^2}\left(1-\frac{\xi_3}{|\boldsymbol{\xi}|}\right) & -\frac{\xi_1}{|\boldsymbol{\xi}|} \\ \frac{-\xi_1\xi_2}{\xi_1^2+\xi_2^2}\left(1-\frac{\xi_3}{|\boldsymbol{\xi}|}\right) & \frac{\xi_3}{|\boldsymbol{\xi}|} + \frac{\xi_1^2}{\xi_1^2+\xi_2^2}\left(1-\frac{\xi_3}{|\boldsymbol{\xi}|}\right) & -\frac{\xi_2}{|\boldsymbol{\xi}|} \\ \frac{\xi_1}{|\boldsymbol{\xi}|} & \frac{\xi_2}{|\boldsymbol{\xi}|} & \frac{\xi_3}{|\boldsymbol{\xi}|} \end{bmatrix}. \tag{A.9}$$

Hence each component of $\boldsymbol{M}_\delta(\boldsymbol{\xi})$ is written as

$$\begin{aligned}[\boldsymbol{M}_\delta^B(\boldsymbol{\xi})]_{ik} &= \int_{B_\delta} \rho_\delta(|\boldsymbol{s}|)\frac{1-\cos(|\boldsymbol{\xi}|s_3)}{|\boldsymbol{s}|^2}\sum_{j=1}^3 \mathcal{R}_{ji}s_j \sum_{l=1}^3 \mathcal{R}_{lk}s_l\, d\boldsymbol{s}, \\ &= \int_{B_\delta} \rho_\delta(|\boldsymbol{s}|)\frac{1-\cos(|\boldsymbol{\xi}|s_3)}{|\boldsymbol{s}|^2}\sum_{j=1}^3 \mathcal{R}_{ji}\mathcal{R}_{jk}s_j^2\, d\boldsymbol{s}, \quad \text{for } i, k = 1, 2, 3,\end{aligned}$$

where $\mathcal{R}_{ij}$ is the component of $\boldsymbol{\mathcal{R}}$. We can rewrite the Fourier symbol $\boldsymbol{M}_\delta^B(\boldsymbol{\xi})$ as

$$\boldsymbol{M}_\delta^B(\boldsymbol{\xi}) = \int_{B_\delta(\boldsymbol{0})} \rho_\delta(|\boldsymbol{s}|)\frac{1-\cos(|\boldsymbol{\xi}|s_3)}{|\boldsymbol{s}|^2}\boldsymbol{M}(\boldsymbol{\xi}, \boldsymbol{s})\, d\boldsymbol{s}, \tag{A.10}$$

where each component of $\boldsymbol{M}(\boldsymbol{\xi}, \boldsymbol{s})$ is given by

$$M_{ik} = \sum_{j=1}^3 R_{ji}R_{jk}s_j^2.$$

From Eq. (A.9), we arrive at

$$\begin{aligned}\boldsymbol{M}(\boldsymbol{\xi}, \boldsymbol{s}) &= \frac{1}{|\boldsymbol{\xi}|^2}\begin{bmatrix} (\xi_2^2+\xi_3^2)s_1^2 + \xi_1^2 s_3^2 & \xi_1\xi_2(s_3^2 - s_1^2) & \xi_1\xi_3(s_3^2 - s_1^2) \\ \xi_2\xi_1(s_3^2 - s_1^2) & (\xi_1^2+\xi_3^2)s_1^2 + \xi_2^2 s_3^2 & \xi_2\xi_3(s_3^2 - s_1^2) \\ \xi_3\xi_1(s_3^2 - s_1^2) & \xi_3\xi_2(s_3^2 - s_1^2) & (\xi_1^2+\xi_2^2)s_1^2 + \xi_3^2 s_3^2 \end{bmatrix}, \\ &= s_1^2\left(\boldsymbol{I}_3 - \vec{\boldsymbol{\xi}}\vec{\boldsymbol{\xi}}^T\right) + s_3^2\vec{\boldsymbol{\xi}}\vec{\boldsymbol{\xi}}^T,\end{aligned} \tag{A.11}$$

where we have used the symmetry of the ball and the equivalence of s_1 and s_2 in the integrand. Substitute Eq. (A.11) into Eq. (A.10), we obtain the second line of Eq. (A.4), and $p_\delta(|\boldsymbol{\xi}|)$ and $q_\delta(|\boldsymbol{\xi}|)$ as given in Eqs. (A.6) and (A.7). □

With the establishment of the previous lemma, we now can prove Lemma 4.2.

Proof of Lemma 4.2. Due to the scaling of the nonlocal kernel Eq. (2), we can rewrite $p_\delta(|\boldsymbol{\xi}|)$, $q_\delta(|\boldsymbol{\xi}|)$ and $b_\delta(|\boldsymbol{\xi}|)$ as the following

$$p_\delta(|\boldsymbol{\xi}|) = \frac{p_1(\delta|\boldsymbol{\xi}|)}{\delta^2}, \tag{A.12}$$

$$q_\delta(|\boldsymbol{\xi}|) = \frac{q_1(\delta|\boldsymbol{\xi}|)}{\delta^2}, \tag{A.13}$$

$$b_\delta(|\boldsymbol{\xi}|) = \frac{b_1(\delta|\boldsymbol{\xi}|)}{\delta}, \tag{A.14}$$

where $p_1(\delta|\boldsymbol{\xi}|)$, $q_1(\delta|\boldsymbol{\xi}|)$ and $b_1(\delta|\boldsymbol{\xi}|)$ are given as in Eqs. (35)–(37) respectively. Combining Eqs. (A.1)–(A.3), we arrive at Eq. (31). Substituting Eqs. (A.12) and (A.13) into Eqs. Eq. (A.4), (A.14) into Eq. (A.5), we obtain Eq. (32). □

A.2. *Proof of Lemma 4.5*

Using Eq. (31) and Parseval's identity, we arrive at

$$\begin{aligned}
((\boldsymbol{u_k}\,\Psi_{\boldsymbol{k}}), -\mathcal{L}_\delta^S(\boldsymbol{v_{k'}}\,\Psi_{\boldsymbol{k'}})) &= (2\pi)^{-\mathrm{d}}\int_{\mathbb{R}^\mathrm{d}} \left(\boldsymbol{u_k}\,\widehat{\Psi_{\boldsymbol{k}}}(\boldsymbol{\xi})\right)\cdot\left(\overline{\boldsymbol{M}_\delta^S(\boldsymbol{\xi})\boldsymbol{v_{k'}}\,\widehat{\Psi_{\boldsymbol{k'}}}(\boldsymbol{\xi})}\right)d\boldsymbol{\xi},\\
&= (2\pi)^{-\mathrm{d}}\int_{\mathbb{R}^\mathrm{d}} e^{i(\boldsymbol{x_{k'}}-\boldsymbol{x_k})\cdot\boldsymbol{\xi}}\left|\widehat{\Psi_{\boldsymbol{0}}}(\boldsymbol{\xi})\right|^2 \boldsymbol{u}_{\boldsymbol{k}}^T\boldsymbol{M}_\delta^S(\boldsymbol{\xi})\boldsymbol{v_{k'}}d\boldsymbol{\xi},\\
&= (2\pi)^{-\mathrm{d}}\int_{\boldsymbol{Q}} e^{i(\boldsymbol{k'}-\boldsymbol{k})\cdot\boldsymbol{\xi}}\,\boldsymbol{u}_{\boldsymbol{k}}^T\boldsymbol{M}_G(\delta,\boldsymbol{h},\boldsymbol{\xi})\boldsymbol{v_{k'}}d\boldsymbol{\xi},
\end{aligned}$$

where we have used Eq. (25) and the Fourier transform of the RK shape function

$$\widehat{\Psi_{\boldsymbol{0}}}(\boldsymbol{\xi}) = \prod_{j=1}^{\mathrm{d}}\widehat{\phi\left(\frac{x_j}{2h_j}\right)}(\xi_j) = \prod_{j=1}^{\mathrm{d}} h_j\left(\frac{\sin(h_j\xi_j/2)}{h_j\xi_j/2}\right)^4,$$

where the Fourier transform of the cubic B-spline function is given as

$$\widehat{\phi}(\xi) = \frac{1}{2}\left(\frac{\sin(\xi/4)}{\xi/4}\right)^4.$$

Hence, the Galerkin form Eq. (38) can be written as

$$\begin{aligned}
(i^h(\boldsymbol{u_k}), -\mathcal{L}_\delta^S i^h(\boldsymbol{v_k})) &= \sum_{\boldsymbol{k},\boldsymbol{k'}\in\mathbb{Z}^\mathrm{d}}\left(\boldsymbol{u_k}\,\Psi_{\boldsymbol{k}}, -\mathcal{L}_\delta^S(\boldsymbol{v_{k'}}\,\Psi_{\boldsymbol{k'}})\right)\\
&= (2\pi)^{-\mathrm{d}}\sum_{\boldsymbol{k},\boldsymbol{k'}\in\mathbb{Z}^\mathrm{d}}\int_{\boldsymbol{Q}} e^{i(\boldsymbol{k'}-\boldsymbol{k})\cdot\boldsymbol{\xi}}\,\boldsymbol{u}_{\boldsymbol{k}}^T\boldsymbol{M}_G(\delta,\boldsymbol{h},\boldsymbol{\xi})\boldsymbol{v_{k'}}d\boldsymbol{\xi}\\
&= (2\pi)^{-\mathrm{d}}\int_{\boldsymbol{Q}}\widetilde{\boldsymbol{u}}(\boldsymbol{\xi})\cdot\boldsymbol{M}_G(\delta,\boldsymbol{h},\boldsymbol{\xi})\overline{\widetilde{\boldsymbol{v}}(\boldsymbol{\xi})}d\boldsymbol{\xi},
\end{aligned}$$

and we have proved (i).

Next, we use the inverse Fourier transform to write

$$
\begin{aligned}
\left(-\mathcal{L}_\delta^S(\boldsymbol{v}_{\boldsymbol{k}'}\Psi_{\boldsymbol{k}'})\right)(\boldsymbol{x}_{\boldsymbol{k}}) &= (2\pi)^{-\mathrm{d}}\int_{\mathbb{R}^{\mathrm{d}}} e^{i\boldsymbol{x}_{\boldsymbol{k}}\cdot\boldsymbol{\xi}}\boldsymbol{M}_\delta^S(\boldsymbol{\xi})\boldsymbol{v}_{\boldsymbol{k}'}\widehat{\Psi_{\boldsymbol{k}'}}(\boldsymbol{\xi})d\boldsymbol{\xi},\\
&= (2\pi)^{-\mathrm{d}}\int_{\mathbb{R}^{\mathrm{d}}} e^{i(\boldsymbol{x}_{\boldsymbol{k}}-\boldsymbol{x}_{\boldsymbol{k}'})\cdot\boldsymbol{\xi}}\boldsymbol{M}_\delta^S(\boldsymbol{\xi})\boldsymbol{v}_{\boldsymbol{k}'}\widehat{\Psi_{\boldsymbol{0}}}(\boldsymbol{\xi})d\boldsymbol{\xi},\\
&= (2\pi)^{-\mathrm{d}}\prod_{j=1}^{\mathrm{d}}(h_j)^{-1}\int_{\boldsymbol{Q}} e^{i(\boldsymbol{k}-\boldsymbol{k}')\cdot\boldsymbol{\xi}}\boldsymbol{M}_C(\delta,\boldsymbol{h},\boldsymbol{\xi})\boldsymbol{v}_{\boldsymbol{k}'}d\boldsymbol{\xi},
\end{aligned}
$$

then we arrive at the collocation form Eq. (39) as

$$
\begin{aligned}
&\left((\boldsymbol{u}_{\boldsymbol{k}}), -r^h\mathcal{L}_\delta^S i^h(\boldsymbol{v}_{\boldsymbol{k}})\right)_{l^2} = \prod_{j=1}^{\mathrm{d}} h_j \sum_{\boldsymbol{k},\boldsymbol{k}'\in\mathbb{Z}^{\mathrm{d}}} \boldsymbol{u}_{\boldsymbol{k}}\cdot\left(-\mathcal{L}_\delta^S(\boldsymbol{v}_{\boldsymbol{k}'}\Psi_{\boldsymbol{k}'})\right)(\boldsymbol{x}_{\boldsymbol{k}})\\
&= (2\pi)^{-\mathrm{d}}\sum_{\boldsymbol{k},\boldsymbol{k}'\in\mathbb{Z}^{\mathrm{d}}}\boldsymbol{u}_{\boldsymbol{k}}\cdot\int_{\boldsymbol{Q}} e^{i(\boldsymbol{k}-\boldsymbol{k}')\cdot\boldsymbol{\xi}}\boldsymbol{M}_C(\delta,\boldsymbol{h},\boldsymbol{\xi})\boldsymbol{v}_{\boldsymbol{k}'}d\boldsymbol{\xi}\\
&= (2\pi)^{-\mathrm{d}}\int_{\boldsymbol{Q}}\widetilde{\boldsymbol{u}}(\boldsymbol{\xi})\cdot\boldsymbol{M}_C(\delta,\boldsymbol{h},\boldsymbol{\xi})\overline{\widetilde{\boldsymbol{v}}(\boldsymbol{\xi})}d\boldsymbol{\xi}.
\end{aligned}
$$

This finishes the proof of (ii). Notice that $\boldsymbol{M}_\delta^B$ and $\boldsymbol{M}_\delta^D$ are positive semidefinite matrices from the assumption $\lambda \geq \mu$. Then (iii) is a result of the direct comparison of Eqs. (40) and (41).

References

[1] S.A. Silling, Reformulation of elasticity theory for discontinuities and long-range forces, J. Mech. Phys. Solids 48 (1) (2000) 175–209.

[2] S.A. Silling, M. Epton, O. Weckner, J. Xu, E. Askari, Peridynamic states and constitutive modeling, J. Elasticity 88 (2) (2007) 151–184.

[3] F. Bobaru, Y.D. Ha, W. Hu, Damage progression from impact in layered glass modeled with peridynamics, Cent. Eur. J. Eng. 2 (4) (2012) 551–561.

[4] Y.D. Ha, F. Bobaru, Studies of dynamic crack propagation and crack branching with peridynamics, Int. J. Fract. 162 (1–2) (2010) 229–244.

[5] H. Ouchi, A. Katiyar, J.T. Foster, M.M. Sharma, et al., A peridynamics model for the propagation of hydraulic fractures in naturally fractured reservoirs, SPE J. 22 (04) (2017) 1082–1102.

[6] M. D'Elia, Q. Du, M. Gunzburger, Recent progress in mathematical and computational aspects of peridynamics, in: G.Z. Voyiadjis (Ed.), Handbook of Nonlocal Continuum Mechanics for Materials and Structures, Springer International Publishing, 2017, pp. 1–26.

[7] Q. Du, M. Gunzburger, R.B. Lehoucq, K. Zhou, Analysis of the volume-constrained peridynamic Navier equation of linear elasticity, J. Elasticity 113 (2) (2013) 193–217.

[8] Q. Du, M. Gunzburger, R.B. Lehoucq, K. Zhou, A nonlocal vector calculus, nonlocal volume-constrained problems, and nonlocal balance laws, Math. Models Methods Appl. Sci. 23 (03) (2013) 493–540.

[9] T. Mengesha, Q. Du, The bond-based peridynamic system with Dirichlet-type volume constraint, Proc. R. Soc. Edinburgh A 144 (1) (2014) 161–186.

[10] T. Mengesha, Q. Du, Nonlocal constrained value problems for a linear peridynamic Navier equation, J. Elasticity 116 (1) (2014) 27–51.

[11] F. Bobaru, J.T. Foster, P.H. Geubelle, S.A. Silling, Handbook of Peridynamic Modeling, CRC Press, 2016.

[12] Q. Du, L. Ju, L. Tian, K. Zhou, A posteriori error analysis of finite element method for linear nonlocal diffusion and peridynamic models, Math. Comp. 82 (284) (2013) 1889–1922.

[13] R.W. Macek, S.A. Silling, Peridynamics via finite element analysis, Finite Elem. Anal. Des. 43 (15) (2007) 1169–1178.

[14] M. Pasetto, Y. Leng, J.-S. Chen, J.T. Foster, P. Seleson, A reproducing kernel enhanced approach for peridynamic solutions, Comput. Methods Appl. Mech. Engrg. 340 (2018) 1044–1078.

[15] P. Seleson, Q. Du, M.L. Parks, On the consistency between nearest-neighbor peridynamic discretizations and discretized classical elasticity models, Comput. Methods Appl. Mech. Engrg. 311 (2016) 698–722.

[16] P. Seleson, D.J. Littlewood, Convergence studies in meshfree peridynamic simulations, Comput. Math. Appl. 71 (11) (2016) 2432–2448.

[17] S.A. Silling, E. Askari, A meshfree method based on the peridynamic model of solid mechanics, Comput. Struct. 83 (17–18) (2005) 1526–1535.

[18] X. Tian, Q. Du, Asymptotically compatible schemes and applications to robust discretization of nonlocal models, SIAM J. Numer. Anal. 52 (4) (2014) 1641–1665.

[19] N. Trask, H. You, Y. Yu, M.L. Parks, An asymptotically compatible meshfree quadrature rule for nonlocal problems with applications to peridynamics, Comput. Methods Appl. Mech. Engrg. 343 (2019) 151–165.

[20] Q. Du, Nonlocal Modeling, Analysis, and Computation, in: CBMS-NSF Conference Series in Applied Mathematics, vol. 94, SIAM, Philadelphia, 2019.

[21] X. Tian, Q. Du, Analysis and comparison of different approximations to nonlocal diffusion and linear peridynamic equations, SIAM J. Numer. Anal. 51 (6) (2013) 3458–3482.

[22] X. Tian, Q. Du, Asymptotically compatible schemes for robust discretization of parametrized problems with applications to nonlocal models, SIAM Rev. 62 (1) (2020) 199–227.

[23] X. Chen, M. Gunzburger, Continuous and discontinuous finite element methods for a peridynamics model of mechanics, Comput. Methods Appl. Mech. Engrg. 200 (9–12) (2011) 1237–1250.

[24] M. D'Elia, M. Gunzburger, C. Vollmann, A cookbook for finite element methods for nonlocal problems, including quadrature rules and approximate Euclidean balls, 2020, arXiv:2005.10775.

[25] Q. Du, Y. Tao, X. Tian, J. Yang, Asymptotically compatible discretization of multidimensional nonlocal diffusion models and approximation of nonlocal Green's functions, IMA J. Numer. Anal. 39 (2) (2018) 607–625.

[26] P. Seleson, Improved one-point quadrature algorithms for two-dimensional peridynamic models based on analytical calculations, Comput. Methods Appl. Mech. Engrg. 282 (2014) 184–217.

[27] K. Yu, X. Xin, K. Lease, A new adaptive integration method for the peridynamic theory, Modelling Simulation Mater. Sci. Eng. 19 (4) (2011) 045003.

[28] F. Xu, M. Gunzburger, J. Burkardt, A multiscale method for nonlocal mechanics and diffusion and for the approximation of discontinuous functions, Comput. Methods Appl. Mech. Engrg. 307 (2016) 117–143.

[29] Y. Leng, X. Tian, N. Trask, J.T. Foster, Asymptotically compatible reproducing kernel collocation and meshfree integration for nonlocal diffusion, 2019, arXiv preprint arXiv:1907.12031.

[30] M. Costabel, F. Penzel, R. Schneider, Error analysis of a boundary element collocation method for a screen problem in $\mathbb{R}^3$, Math. Comp. 58 (198) (1992) 575–586.

[31] D.N. Arnold, J. Saranen, On the asymptotic convergence of spline collocation methods for partial differential equations, SIAM J. Numer. Anal. 21 (3) (1984) 459–472.

[32] D.N. Arnold, W.L. Wendland, On the asymptotic convergence of collocation methods, Math. Comp. 41 (164) (1983) 349–381.

[33] H.-Y. Hu, J.-S. Chen, S.-W. Chi, Perturbation and stability analysis of strong form collocation with reproducing kernel approximation, Internat. J. Numer. Methods Engrg. 88 (2) (2011) 157–179.

[34] H.-Y. Hu, J.-S. Chen, W. Hu, Error analysis of collocation method based on reproducing kernel approximation, Numer. Methods Partial Differential Equations 27 (3) (2011) 554–580.

[35] J.S. Chen, M. Hillman, S.W. Chi, Meshfree methods: progress made after 20 years, J. Eng. Mech. 143 (4) (2017) 04017001.

[36] S. Li, W.K. Liu, Moving least-square reproducing kernel method part II: Fourier analysis, Comput. Methods Appl. Mech. Engrg. 139 (1–4) (1996) 159–193.

[37] S. Li, W.K. Liu, Synchronized reproducing kernel interpolant via multiple wavelet expansion, Comput. Mech. 21 (1) (1998) 28–47.

[38] S.A. Silling, R.B. Lehoucq, Peridynamic theory of solid mechanics, in: Advances in Applied Mechanics, Vol. 44, Elsevier, 2010, pp. 73–168.

[39] Q. Du, X. Tian, Stability of nonlocal Dirichlet integrals and implications for peridynamic correspondence material modeling, SIAM J. Appl. Math. 78 (3) (2018) 1536–1552.

[40] Q. Du, X. Tian, Mathematics of smoothed particle hydrodynamics: A study via nonlocal Stokes equations, Found. Comput. Math. (2019) 1–26.

[41] H. Lee, Q. Du, Nonlocal gradient operators with a nonspherical interaction neighborhood and their applications, ESAIM Math. Model. Numer. Anal. (2019) in press.

[42] S.A. Silling, R.B. Lehoucq, Convergence of peridynamics to classical elasticity theory, J. Elasticity 93 (1) (2008) 13.

[43] Y. Leng, X. Tian, J.T. Foster, Super-convergence of reproducing kernel approximation, Comput. Methods Appl. Mech. Engrg. 352 (2019) 488–507.

[44] W.K. Liu, S. Jun, Y.F. Zhang, Reproducing kernel particle methods, Int. J. Numer. Methods Fluids 20 (8–9) (1995) 1081–1106.

[45] N. Trask, B. Huntington, D. Littlewood, Asymptotically compatible meshfree discretization of state-based peridynamics for linearly elastic composite materials, 2019, arXiv preprint arXiv:1903.00383.